

Investigation of Surface Roughness and Lay on Metal Flow in Hot Forging

David Joseph Nowak
Marquette University

Recommended Citation

Nowak, David Joseph, "Investigation of Surface Roughness and Lay on Metal Flow in Hot Forging" (2014). *Master's Theses (2009 -)*. Paper 269.
http://epublications.marquette.edu/theses_open/269

**INVESTIGATION OF SURFACE ROUGHNESS AND LAY ON
METAL FLOW IN HOT FORGING**

By

David J. Nowak, B.S.

A Thesis submitted to the faculty of the Graduate School,
Marquette University,
in Partial Fulfillment of the Requirements for
the Degree of Master of Science in Mechanical Engineering

Milwaukee, Wisconsin

August 2014

ABSTRACT
INVESTIGATION OF SURFACE ROUGHNESS AND
LAY ON METAL FLOW IN HOT FORGING

David J. Nowak, B.S.

Marquette University, 2014

A study was conducted to explore the possibility of using machining marks (i.e. surface roughness and lay) as a parameter for die design. The study was performed using 6061-T6 aluminum 1.25" diameter rounds and 0.25" square bar stock to investigate the effects of temperature, surface roughness, and lay on metal flow and friction factor. Metal flow was assessed using component true strains and spread ratio. Compression testing was performed using an instrumented die set that was mounted on a 10 ton hydraulic press. Cigar tests were performed where the axis of the specimen were oriented at angles of 0°, 45° and 90° with respect to the surface lay on the compression platens. Ring tests were completed to quantify friction factor at different die temperatures and surface roughness values. Results indicate that die temperature has a strong effect on bulge radius and friction factor. Lay and surface roughness were found to exhibit an effect on metal flow but surface lay of the dies was not discernible on friction factor. The study was repeated under limited conditions using graphite lubricant in order to discover if the trend was repeatable using conditions observed in industry. This was found to be the case.

Acknowledgements

David J. Nowak, B.S.

I would like to thank everyone that assisted with the research and helped ensure its completion. This includes the help of the Senior Design Students who did a great job designing and building the die set (Messrs. Dan Armstrong, Benjamin Gumieny, Richard Roberts, Edmund Khoo, Kari Nabrzyski). I would also like to thank the Forging Industry Educational and Research Foundation (FIERF) for the opportunity to complete the research and for funding it. The assistance of Mr. Tom Siliman was invaluable in developing the die machining process as well as getting all the specimens machined. Dr. Domblesky was the guiding light throughout the entire processes, making sure I stayed on track and helping out when things did not go according to plan. Without the help of all the graduate students to help run the experiments, I would not have been able to finish when I did. These include Messrs. Charlie Janicki, Joe Segatta, Edgar Espinoza, John Neuman, and Shichao Hu. I also would like to thank my parents, Jeffrey and Jennifer, and my Grandmother for helping me get to where I am today.

TABLE OF CONTENTS

LIST OF FIGURES	IV
LIST OF TABLES	VIII
1. INTRODUCTION	1
2. LITERATURE REVIEW	7
2.1. Overview of Friction in Bulk Metal Forming.....	7
2.2. Friction Testing in Bulk Metal Forming.....	8
2.2.1. Ring Compression Test	8
2.2.2. “Cigar” Test	10
2.2.3. Cylinder Upsetting	11
2.2.4. Other Friction Measurements Methods in Hot Forging.....	14
2.3. Wear Mechanics and the Relationship to Die Roughness	15
2.3.1. Die Conditions and the Relationship to Coefficient of Friction	16
2.3.2. Asperity Based Friction Modeling.....	18
2.3.2.1. Asperities and Lubricant Interaction.....	20
2.4. Surface Roughness and the Relationship to Friction Models.....	21
2.4.1. Surface Roughness and its Orientation with respect to the Work piece	22
2.5. Friction Relationships Found in Other Bulk Deformation Processes.....	24
3. EXPERIMENTAL SETUP	29
3.1. Press Setup & Die Tooling	29

3.2. Die Machining Procedure Used to Achieve Controlled Surface Topography	33
3.2.1. Platens Used for Cigar Test	34
3.2.2. Platen Machining Used for Cylindrical Upset Testing	39
3.3. Work Piece Material and Geometry	40
3.4. Summary of Experimental Methodologies	41
3.4.1. Cylindrical Upsetting Test Methodology	41
3.4.2. Cigar Test Methodology.....	43
3.4.3. Ring Compression Test Methodology.....	45
4. DISCUSSION & RESULTS.....	48
4.1. Cylindrical Upset Testing Results	48
4.2. Cigar Testing Results and Discussion	51
4.2.1. Effect of Surface Roughness on True Strain	53
4.2.1.1. Un-Lubricated Tests	53
4.2.1.2. With Lubricant	56
4.2.2. Comparison of True Strain to Part Lay/Orientation	59
4.2.2.1. Un-Lubricated Results	60
4.2.2.2. Testing With Lubricant.....	68
4.2.3. DEFORM Finite Element Analysis	73
4.3. Ring Testing Results and Discussion.....	78
4.3.1. Dry Results	78
4.3.2. Lubricant Results.....	81
5. SUMMARY AND CONCLUSIONS.....	82

6. RECOMMENDATIONS FOR FUTURE WORK	84
7. REFERENCES	86
8. APPENDICES	89
Appendix A - Cigar Test Results Examining part orientation with respect to material flow without lubricant.....	89
Appendix B - Cigar Test Results Examining Surface Roughness with respect to material flow with lubricant	91
Appendix C - Calculated Standard Deviations for the Collected Data.....	93

LIST OF FIGURES

Figure 1.1 - Surface texture features found on surfaces. (After Ref. [1]).....	2
Figure 2.1 - Plot of friction against roughness shows a negative slope region caused by excessive junction growth, and a positive region caused by interlocking of asperities. In between, friction is independent of roughness. (After Ref. [17])	18
Figure 3.1 - Photo showing the Technovate press with die set, data acquisition, and temperature controllers mounted.	30
Figure 3.2 - Close up view of the experimental die setup used in the investigation with key parts labeled.....	30
Figure 3.3 - Block diagram of instrumentation and PID controllers used on the hydraulic press and die set.	32
Figure 3.4 - Schematic showing different specimen orientations used to assess the effect of part lay .From left to right, the longitudinal orientations of the specimens are, 90°, 45°, and 0° (parallel) with respect to the surface roughness.	35
Figure 3.5 - Close up view of the grooves on the 125- μ in R_a die after machining. The magnification is 400x.....	37
Figure 3.6 -A schematic of the 125 micro-inch R_a platen surface after machining. All dimensions are in inches.	38
Figure 3.7 -A schematic of the 250 micro-inch R_a platen surface after machining. All dimensions are in inches.	38
Figure 3.8 - A schematic of a ring test specimen on the machined die platen with concentric lay. The arrows indicate the direction that the point will flow. Note how the arrows intersect the machined pattern at perpendicular angles.	40
Figure 3.9- A top view of the various specimens used in the study. From left to right: A.) cylindrical specimen B.) rectangular specimen and C.) ring compression test specimen.....	41
Figure 3.10 -A cylindrical specimen shown after compression. Note the bulged sides.....	42

Figure 3.11 - Plane views of representative forged prismatic specimens with the width and length Dimension, w and l respectively, indicated. The orientation of each specimen is discernible from the lines on the surface of each specimen.	45
Figure 3.12 - A schematic of a ring test specimen on the machined die platen with directional lay. The arrows indicate direction that the point will flow. Note how the arrows intersect the machined pattern at angles varying from 0 to 90 degrees.	47
Figure 4.1 - Radius of curvature plotted as a function of die temperature for 6061-T6 cylindrical specimens	50
Figure 4.2 – Average length strain as a function of surface roughness for the rectangular specimens. Tests were performed without lubrication.....	54
Figure 4.3 – Average width strain as a function of surface roughness for the rectangular specimens. Tests were performed without lubrication.	55
Figure 4.4 - Average spread ratio as a function of surface roughness for rectangular specimens. Tests were performed without lubrication.	56
Figure 4.5 – Average length strain as a function of surface roughness for rectangular specimens. Tests were performed with lubrication.....	57
Figure 4.6 – Average width strain as a function of surface roughness for rectangular specimens. Tests were performed with lubrication.....	58
Figure 4.7 - Average spread ratio as a function of surface roughness for rectangular specimens. Tests were performed with lubrication.....	59
Figure 4.8 - Average length strain as a function of part orientation for smoother dies. Tests were performed without lubrication.....	60
Figure 4.9 - Average length strain as a function of part orientation for rougher dies. Tests were performed without lubrication.	61
Figure 4.10 - Average width strain as a function of part orientation for smoother dies. Tests were performed without lubrication.....	62
Figure 4.11 - Average width strain as a function of part orientation for rougher dies. Tests were performed without lubrication.	62
Figure 4.12 - Average spread ratio as a function of part orientation for smoother dies. Tests were performed without lubrication.....	64

Figure 4.13 - Average spread ratio as a function of part orientation for rougher dies. Tests were completed preformed lubrication.....	65
Figure 4.14 – A close-up die view showing a cigar specimen and the arrow showing the width flow direction at 0 Degrees (Long axis parallel to grooves). Note that the darkened region represents a very close detailed side top view of the cigar specimen.....	66
Figure 4.15 - A close-up die view showing a cigar specimen and the arrow showing the width flow direction at 45 Degrees. Note that the darkened region represents a very close detailed side top view of the cigar specimen.....	67
Figure 4.16 - A close-up die view showing a cigar specimen and the arrow showing the width flow direction at 90 degrees (Long Axis Perpendicular to Grooves). Note that the darkened region represents a very close detailed side top view of the cigar specimen.....	67
Figure 4.17 - Average length strain as a function of part orientation for smoother dies. Tests were performed with lubrication for the rectangular specimens.....	69
Figure 4.18 – Average length true strain as a function of part orientation for rougher dies. Tests were performed with lubrication for the rectangular specimens.....	69
Figure 4.19 - Average width strain as a function of part orientation for smoother dies. Tests were performed with lubrication.....	70
Figure 4.20 - Average width true strain as a function of part orientation for rougher dies. Tests were preformed with lubrication.	71
Figure 4.21 - Average spread ratio as a function of part orientation for smoother dies. Tests were preformed with lubrication.....	72
Figure 4.22 - Average spread ratio as a function of part orientation for rougher dies. Tests were preformed with lubrication.	73
Figure 4.23 – Two-dimensional, plane strain, non-isothermal FE model of the cigar test with surface roughness of 125 μin platens. The line to the left of the model represents the centerline of the part and a plane of symmetry.	74
Figure 4.24 - The DEFORM model after deformation was complete.	75
Figure 4.25 – Velocity field results from DEFORM 2D of cigar specimen orientated at 0 degrees. The same coordinate axis is shown in the lower right of the group of pictures. The model progresses alphabetically (a	

through e) and show the progress of the specimen bridging the groove in the X direction and then curling upwards in the Y direction.	76
Figure 4.26 – 10X magnification of a cross section of a cigar test specimen. There appears to be some curl in the noted area.	78
Figure 4.27 - Ring compression test results shown as friction factor as a function of die temperature completed on a 60 μ in R_a concentric die.	79
Figure 4.28 - Ring compression test results shown as friction factor as a function of die surface roughness at 400°F die temperature. Performed in the dry condition (No Lubricant).	80
Figure 4.29 - Ring compression test results show as friction factor as a function of die surface roughness at 400°F die temperature. Completed using lubricant.	82
Figure 8.1 – Combined length true strain plotted as a function of part orientation in the dry state.	89
Figure 8.2 - Combined width true strain plotted as a function of part orientation in the dry state.	90
Figure 8.3 - Combined spread ratio plotted as a function of part orientation in the dry state.	90
Figure 8.4 - Combined length true strain plotted as a function of part orientation completed with lubricant.	91
Figure 8.5 – Combined width true strain plotted as a function of part orientation completed with lubricant.	91
Figure 8.6 – Combined spread ratio plotted as a function of part orientation completed with lubricant.	92

LIST OF TABLES

Table 1 - Summary of conditions used for a portion of the temperature study. The test consisted of cylindrical specimens upset at the listed temperatures and the resulting bulge radius measured. Note that this test was completed without lubricant.	43
Table 2 - Summary of conditions used for cigar testing. The test investigated material flow with respect to part lay and was completed and without lubricant.	44
Table 3 - Summary of conditions used for a portion of the temperature study. Ring specimens were upset at the listed temperatures and the resulting friction factor measured. No lubricant was used for this portion of the test. These tests are represented schematically in Figure 3.8.....	46
Table 4 - Summary of conditions used for the study of surface roughness with respect to friction factor. Ring specimens were upsets at the listed surface roughness values while the temperature was held constant. Tests were performed with and without lubricant. These tests are represented schematically in Figure 3.12.....	46
Table 5 - Calculated sample standard deviation for each trial of the study.....	93

1. Introduction

In hot forging operations, a key challenge facing forging engineers is how to optimize a die design to achieve complete fill and attain reasonable die life. While it is accepted that friction has an effect on both die fill and life, conventional wisdom in forging practice holds that friction is detrimental and should be minimized to promote material flow and improve die life. However, this implies that friction can also be used to inhibit flow. The ability to promote, or inhibit, flow suggests that friction could represent a potential die design parameter, and it is hypothesized in the present study that it might also be used as a means to locally control material flow in the die cavity. For example, a forging engineer might specify a rougher surface in one area on the die surface to retard flow such that a different region, for example a corner having a smoother surface, promotes material flow and fills preferentially. It should be noted that this is not intended to replace the flash land but rather, to potentially supplement it as a means to facilitate die fill on a local level.

Although it can be argued that friction represents a second order effect in a forging operation, an improved understanding of the role it plays would help to provide increased process control as well as assessing its potential as a tool for controlling metal flow. While friction is determined by a number of factors, surface topography is considered to be a key parameter. Surface topography is composed of many components that include the height and width of roughness, lay directions, and waviness, all of which are shown below in Figure 1.1. As such, the overall goal of this investigation is to

determine how significant of an effect that die topography, specifically surface roughness and its orientation (lay), have on material flow in hot forging.

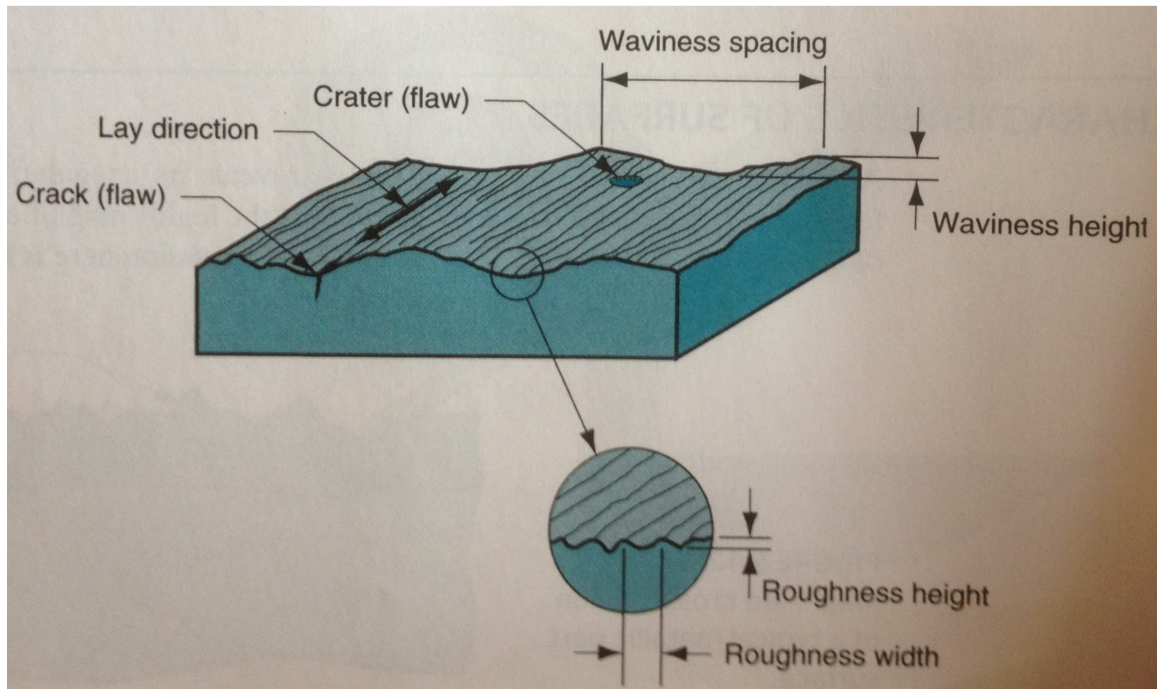


Figure 1.1 - Surface texture features found on surfaces. (After Ref. [1])

If a correlation can be drawn between surface roughness/lay and metal flow, this could also contribute to development of a more comprehensive friction model for metal forging that accounts for surface geometry. Friction modeling improvements could advance die design by optimizing wear and heat patterns within the die leading to longer die life and facilitating die fill. Because friction is known to be sensitive to temperature as well as surface topography, it is also of interest to investigate the linkage between forging die roughness and temperature as part of a potential control strategy.

A review of the metal forming literature shows that most of the friction related research that has been published to date, including studies related to die/work piece

surface interactions, has focused primarily on cold working processes. Cold forming is generally defined as plastically deforming a metal at less than 30% of its absolute melting temperature. In comparison, hot forging occurs when the working condition is above the material's recrystallization temperature (i.e. 50% of the absolute melting temperature or higher). Cold forging is generally limited to smaller, axisymmetric, net-shape parts, such as steel fasteners and aluminum carabineers. This limitation is primarily due to the high pressures and forces needed to plastically deform material into complex shapes and reduced workability at lower temperatures.

More complex geometries necessitate heating the material and working it above the recrystallization temperature to ensure adequate material flow and reasonable die pressures. The vast majority of parts made by bulk forming utilize a hot forging process, which permits greater geometric complexity as well as placing fewer restrictions on part size. An added benefit of hot working is improved material ductility and better ability to control the microstructure within the part. However, from a research perspective, cold forming has fewer variables, and, therefore, is more controllable and repeatable. In comparison, hot forging poses a greater challenge as it requires the ability to exercise a high degree of control over the temperatures of both the work piece material and die surfaces. In spite of these challenges, more research into the effects of die and work piece friction on metal flow at elevated temperatures would be beneficial given the wider utilization of hot forming processes for commercial parts.

Friction effects in forging are usually represented mathematically as an interfacial shear stress using one of two possible models. The Coulombic model has traditionally been used in metal forming where friction is considered to be proportional to the normal

pressure applied to a surface. The second model is termed the interface friction factor, or friction factor for short. In this model friction is represented as a percentage of the material's shear yield strength. Most forging operations require high pressures, due to the severity of deformation and material flow required. However, for coefficients of friction greater than 0.577, the high pressures caused by forging often result in an artificially high value of interfacial shear stress. In a real metal, the maximum shear stress must be less than or equal to half of the yield strength in order to be consistent with established yield criteria. This inconsistency explains why use of the friction factor is often preferred in forging as it is based on the fact that when the material adheres or is "welded" to a surface, the subsurface layers will plastically deform by shear.

As noted earlier, friction is usually viewed as having a negative effect in forging processes and efforts are normally made to minimize it. Applying lubricants to the die surface is one of the most common practices that forgers use to minimize friction. The role of the lubricant is to promote metal flow by creating a mixed boundary layer that helps to separate the work piece and die surfaces. In addition to reducing friction, the work piece will also have a better surface finish as a result. Another method that is used to reduce friction and increase die life is by controlling the surface roughness of the dies. Anecdotally, the forging industry tries to keep average surface finish on dies below an average surface roughness, R_a or R_{RMS} , of 60 μin , but above a certain roughness threshold, usually 20 μin . It should be noted that having too smooth of a surface, which theoretically would reduce friction to a minimum, actually reduces lubricant retention on the die, and results in greater metal-to-metal contact at the interface. The loss of lubricant

and increased metal contact results in increased die wear which is contradictory to what forging engineers are trying to achieve.

The purpose of this thesis is to investigate how die surface topology, specifically roughness and its orientation, affects metal flow in hot forging. The study was structured to include two parts. The first was to experimentally study the effects of die temperature and surface topography (i.e. roughness and lay) and to consider the phenomenon that are involved. This experiment involved compression testing of cylindrical specimens to understand how die temperature affected the friction factor when die roughness and specimen temperature were held constant. The second experimental study was conducted by varying part orientation with respect to lay (i.e. directionality of machining marks) at fixed values of surface roughness. Five different surface roughnesses were used to encompass the range of values that would be encountered in a typical forging die. The temperature of the dies and specimens were held constant for this study to minimize the number of confounded variables. The second part additionally included using DEFORM, a commercial Finite Element Analysis program used to simulate the forging processes. Simulations were conducted in an effort to understand and visualize how material flow occurred in the vicinity of the die/part interface at one particular orientation.

The research that was conducted is expected to contribute to both fundamental metal working knowledge and forging industry practice. From a fundamental perspective, the research will help to provide additional insight regarding the relationship between friction, surface topography, and metal flow. Currently, topography of a die surface that results from die machining is not taken into account when calculating friction. The aim of the research is to explore if the surface topography of a die is an influential factor on

material flow and will indirectly contribute to an understanding of how manufacturing methods impact the process. The work laid out in this research will help establish if friction is influenced by a work piece's orientation with respect to a die's surface. This is contrast to the current understanding, where friction is considered to be constant regardless of the direction of metal flow.

With respect to forging practice, this research can help lead to new die design and analysis methods. A better understanding of how surface roughness affects metal flow can aid in creating more refined friction models that reflect local values based on die surface roughness measurements, as well as how worn or rougher areas can affect metal flow. Additionally, based on information gained in the study of part lay with respect to surface roughness, a beneficial effect in enhancing lubrication performance and minimizing or maximizing resistance to material flow of the work piece might be discovered. If these factors are combined with others used in forging, such as lubrication selection and flash land locations within a die, part lay and roughness might help to realize the next phase of die design which is related to surface engineering.

2. Literature Review

An examination of the literature related to friction in forging shows that much of the research work that has been conducted has been focused on cold forming operations. As noted in Chapter 1, this is attributed in part to the fact that fewer variables need to be controlled and results are more reproducible in comparison to hot forging. While application of findings from cold forming studies to a hot forging process need to account for the difference in temperature, there is still some merit in reviewing the existing literature on tribology and friction since the metal flow mechanisms and pressure magnitude are comparable.

2.1. Overview of Friction in Bulk Metal Forming

One of the more comprehensive discussions of friction in metal forming can be found in John Schey's book titled Tribology in Metalworking [2]. While, Schey presents a broad overview of the topic, there are several key points pertaining to hot forging and frictional effects that are worth noting. In relation to die topography and friction, Schey discusses some of the research that has focused on identifying optimal lubricants or treatments to reduce friction. Schey reviews the use of liquid and solid lubricants, as well as surface treatments such as nitriding, that can be applied to die surfaces to promote metal flow. However, most of the findings are very dependent on process conditions and Schey notes that liquid lubricants have the best performance in both cold and hot forming. This statement is based on the fact that liquids are easier to control when

applying, easier to clean up, and create a hydrodynamic layer between the work piece and die.

Another topic that Schey [2] covers is the design of flash lands in impression forging dies. The intent behind flash lands is to provide extra resistance to prevent metal flow. In particular, flash lands are used to develop a backpressure to cause metal flow to occur in those areas in a die, such as corners, where complete fill is difficult. The backpressure is caused in part by frictional constraints and increased flow stress of the flash. Schey notes that a balance is needed between the depth and width of the flash land in order to promote material chilling within the area. Once metal in the flash land is cooled, its flow stress greatly increases and creates extra resistance to metal flowing out of the die, thus guiding fill in unfilled areas such as corners. The problem is that once the ideal flash land ratio has been achieved, additional die fill cannot be achieved without causing excessive die stress. If the metal still is not flowing into hard to fill cavities after proper flash land sizing, then a modification to the lubricant should be considered. Overall, the use of flash lands is subject to diminishing returns such that other factors must also be considered to further optimize metal flow and also provides support for the current investigation.

2.2. Friction Testing in Bulk Metal Forming

2.2.1. Ring Compression Test

The ring compression test was developed by Male and Cockcroft in the 1960's and has been verified as a robust tool to measure friction between a work piece and die

surfaces. Because of this, the test has wide application to forging practice including, lubricant evaluations [3, 4], the examination of surface roughnesses on dies [5] and the relationship of flow stress and softening at different temperatures and roughnesses [6-8]. In the ring test, a hollow metal cylinder having a fixed ratio of outer diameter: inner diameter: height, usually 6:3:2, is compressed. The resulting change in the outer and inner diameters is then compared to a known set of curves to determine the friction factor [9]. One shortcoming of the method is that friction has to be assumed to be constant in all directions on a surface. For example, if a surface has friction differentials, the resulting ring geometry would be expected to be non-symmetric. The subsequent elliptical shape is difficult to compare against a calibration curve, since the amount of deformation varies from area of the specimen to another, resulting in deviations from these variations being averaged out.

Male and Cockcroft reference the work of Webster and Schroder [10] in the pressing of thin solid disks for their calibration curves. The researchers aimed to model how an increase in friction would change the overall bulk deformation geometry. Webster and Schroder developed a model for the relationship between pressures, friction, and total part deformation using thin uniform disks instead of rings under cold forming conditions. While their work improved understanding of the effect of part diameter and height to its observed friction factor in the ring compression test, they did not explore the consequential bulging of the thin disks caused by friction. The bulging can affect the overall friction factor calculation which means that Webster and Schroder overestimated the amount of deformation in their work. This is attributed to the ideal deformation the researchers assumed in their mathematical model as compared to the actual bulging that

took place in the experiment. Male and Cockcroft used the effects of part width and height explored by Webster and Schroder extensively to develop their calibration curves that are now used as a standard reference. However, both the ring compression test and the thin uniform disk test require a very large frictional coefficient in order to be relatively accurate.

2.2.2. “Cigar” Test

Another test that is used to measure friction in forging applications is the so-called “Cigar Test”. The name results from the fact that after small rectangular slabs are compressed they closely resemble the shape of a cigar. In this test the change of width of the compressed specimen is used to calculate the friction factor between the part and die. This test can be used to measure friction factor, as long as the initial specimen length is at least ten times larger than its width. Due to frictional restraint in the long axis, the specimen will preferentially deform along the direction of the shortest dimension. However, if friction is low enough along the long axis, the length or the longest dimension will also increase which makes it difficult to measure a friction factor using only the change in width. The use of a shorter ratio was however investigated by Fricker and Wanhiem, who used specimens where the length was much less than ten times the width [11], in order to evaluate lubricants at cold working temperatures. However, while they were able to accurately measure very low coefficients of frictions (i.e. coefficients less than 0.05), it should be noted that for higher values the ring compression test has been shown to be more accurate. This accuracy was achieved by using a ratio of the

change of width and length, instead of just the width dimension. Low values of friction coefficients and factors are normally observed in cold forming. In hot forging, friction values are much higher, limiting use of this test with very short length/width ratios test and thus the ring compression test is more commonly used. However, both the cigar test and the ring compression test are not sensitive enough to distinguish between changes in friction factor between an x-direction and y-direction on the die. The present study uses a cigar test ratio less than ten times the width, because the flow in each direction will be used to assess resistance to flow in each direction. This method is an indirect method to measure the friction factor but presents the best test with respect to the options available.

2.2.3. Cylinder Upsetting

Compression of cylindrical specimens parallel to the longitudinal axis, termed upsetting, has also been used to study friction in metal forming. In frictionless upsetting, deformation should proceed in a proportional manner and result in a compressed geometry that is free of any curvature or “bulging”. However, when friction is present, it restricts radial flow at the die interfaces and causes the material to preferentially flow in the mid-section of the part. The constrained flow adjacent to the top and bottom faces creates a “bulging” effect which is proportional to the degree of frictional restraint. Schey, Venner and Takomana [12] attempted to use changes in the height and diameter of a cylinder as a means to predict a friction factor but promote caution based on a complex surface interaction which is termed stick-slip friction. Stick-slip friction occurs when the surface of a specimen moves relative to the dies, but as frictional forces

increase, the specimen will start to adhere or “stick” causing the lateral metal flow to cease. As deformation continues and increased force is applied to the die, the part seemingly becomes un-stuck and resumes flowing. The cyclic nature of the process is caused by the friction regime alternating between static and dynamic friction. If performed using a lubricant, the upsetting test can be more reliable since the lubricant provides a film for the material to flow on, minimizing the stick-slip phenomena. Running the test dry creates issues besides stick-slip, including the need for a large press load to complete the test, as well as accelerated part chilling, since as contact pressures increase, heat transfer increases as well. But this is not to say the compression of a cylinder is not a valid way to measure friction.

Malayappan and Narayanasmy [13] have also investigated the relationship between the bulge diameter of a cylinder and friction factor under cold forming conditions. They hypothesized that bulge diameter (i.e. from the radius of curvature for the bulge) could be used as a means for a relative measure of friction. Different machining techniques were used to achieve a range of surface roughnesses, to vary friction in their experiment. Aluminum cylinders were upset at room temperature to specific true strains ranging from around 0.2 to 0.8. Using an optical comparator, they measured the radius of curvature of the bulge on individual cylindrical specimens, which was then correlated to the friction factor as follows. In order to determine a linear relationship between friction factor and deformation, the bulge radii as a function of hydrostatic stress was plotted with an empirical constant for the shape. The shape constant adjusts for the error created by the assumption that the bulge curvature is a perfect arc. An important point to note is that the roughest die, which had an R_a of 107.48

μin , machined using Electrical Discharge Machining (EDM), produced the most barreling and friction, while a milled die (R_a of $51.964 \mu\text{in}$), showed much lower barreling and friction. The lowest amount of barreling was produced on a ground die with a surface roughness R_a of $0.196 \mu\text{m}$ ($7.7165 \mu\text{in}$). This suggests that friction has a direct correlation to the average surface roughness, R_a .

The upsetting test has also been compared against the ring compression test as a method to determine the friction factor for different lubricants. The calculation is performed by analyzing the deformation of cylindrical and ring specimens using identical conditions to find the actual friction factor encountered. The bulge radius of curvature has been found to have a good correlation to the actual values obtained by the ring compression test as the bulge diameter will decrease with friction factor. This is in agreement with findings from Malayappan and Narayanasamy's previous study. However, the tests were all run at room temperature. Additionally, the study was only a comparison, meaning that they did not develop a direct method to take measurements from the cylinders and calculate a friction factor[14].

Baskaran, Narayanasamy, and Arunachalam [15] conducted a variation of the cold upsetting test by using elliptical rather than cylindrical specimens and different lubricants to vary the friction factor on each die. The authors hypothesized that using a shape that was shorter in one direction would provide greater sensitivity to differences in friction and, by staying with a semi-cylindrical shape, they could use the previously established bulge radius relationship. They were able to achieve differential friction factors by using different lubricants on opposite faces of the elliptical work pieces. Three different minor to major diameter ratios were used as well as various lubricants and upset

strains. Again, a strong correlation was found between the bulge diameter and the friction factor. Similar to their previous two studies, the researchers plotted the bulge radius as a function of hydrostatic stress and fitted a power law relationship. This relationship was then compared against the different friction factors used. They calculated a new shape factor as well, since there was a difference in shape between the elliptical and cylindrical work piece geometries. While they found that there was a correlation between the friction factor and the barreling, they also found that as the minor/major diameter ratios increased, the observed radius of curvature also increased.

2.2.4. Other Friction Measurements Methods in Hot Forging

A study by Li et al. [16] used the bulge radius from cylindrical steel specimens to establish if large strain rates had an effect on the friction factor in hot forging. Steel cylinders were heated to temperatures between 1472° F and 2192° F and then upset to true strains ranging from 0.2 to 1.6. A carbon sheet was placed between the work piece and dies to act as a lubricant as well as an insulator. Mica sheets were also used to provide additional insulation since unheated dies were used. To further minimize die chilling, the experiments were conducted using induction-heating coils to help maintain the work piece temperature. The study was also conducted in a vacuum to minimize scale formation on the work piece. The DEFORM software code was used to back calculate the friction factor based on the bulge radius obtained from experimentation. Based on the results, Li et al. found that friction factor was not constant during large strain rate deformation but showed an increase with strain. The researchers also found that the

friction factor did not demonstrate a strong correlation to the bulge radius when cylinders were upset to high strain values. While the researchers did find a way to calculate an instantaneous friction factor, the large temperature difference between the work piece and the dies caused significant die chilling, even with the insulators in place. The experiment only varied work piece temperature instead of die temperature or surface conditions, which would also be expected to have an effect on friction. While the researchers did demonstrate good agreement between the computer model and the experiment, the results are difficult to use directly in order to improve die design.

2.3. Wear Mechanics and the Relationship to Die Roughness

Related to the investigation of friction in forging, other researchers have considered the wear processes operating on die surfaces. The concentration has been on the abrasion and adhesion wear mechanisms between two materials (a two body wear system), as well as the wear caused by the formation of loose particles (a three body wear system) that cause mechanical deformation and erosion between two surfaces. This is applicable to in the present study as the effect of die wear would be expected to increase the friction factor on the die surface over time and potentially influence flow. In forging practice, worn surfaces tend to be related to high average surface roughness, R_a , such that die topography will tend to roughen as a result of abrasive and adhesive wear. A detailed discussion of abrasion and adhesion can be found in Friction and Wear of Materials by Ernest Rabinowicz [17] which summarizes fundamental work, explains the mechanisms and principles of material wear, and the influence of wear on friction.

Rabinowicz also presents an analysis of lubricants and how they act to reduce wear and friction; though much of this concerns conditions at lower temperature levels and higher sliding speeds than are typically encountered in hot forging. Rabinowicz discusses asperity interaction between two surfaces resulting in a change in frictional resistance, which does have some application to the forging industry.

2.3.1. Die Conditions and the Relationship to Coefficient of Friction

Rabinowicz makes several important points notes in his book that are applicable to the present study. The first is that friction has no clear correlation to temperature. Instead, his contention is that temperature changes the material properties of the moving surfaces, which in turn, reduces the force needed for material to slide. Rabinowicz references work done by Simon, McMahon, and Bowen [18], who used a pin-slider system to examine friction coefficients for different materials at temperatures ranging from -270°C to 300°C . The researchers found no clear correlation between friction and temperature, and instead found the relationship between friction and temperature to be very stable when taking oxide layer formation and surface interaction into account. High pressures were not considered, due to the nature of the pin slider system and as a result the researchers assumed no asperity flattening was taking place. Since higher pressures were not considered, further investigation is warranted to determine whether or not their findings are applicable at forging pressures and conditions.

A second interesting point that Rabinowicz makes is that the relationship between surface roughness and the coefficient of friction is not linear but follows a

parabolic curve [17]. Rabinowicz notes that for very low values of roughness (i.e. RMS 0-10 μin), the coefficient of friction increases as the surface becomes smoother. This data was gathered from a pin on disk test between a copper pin and disk. The inverse relationship between the coefficient of friction and RMS surface roughness for smooth surfaces is explained by the growth in the number of junctions between the work piece and plate, and increased contact area that results as a surface gets “smoother”. The larger contact area results in more heat generation at the interface during sliding which promotes asperity welding and adhesion and acts to create more frictional resistance. From RMS 10-50 μin , there is a relatively stable amount of friction due to a balance between localized micro welding and the force needed to shear large asperity contact areas. Increasing RMS roughness above 50 μin causes an increased coefficient of friction as a result of more asperities interlocking with the work piece material and requiring increased force to shear. Figure 2.1, taken from Rabinowicz, illustrates the relationship between surface roughness and coefficient of friction over a representative range of RMS values.

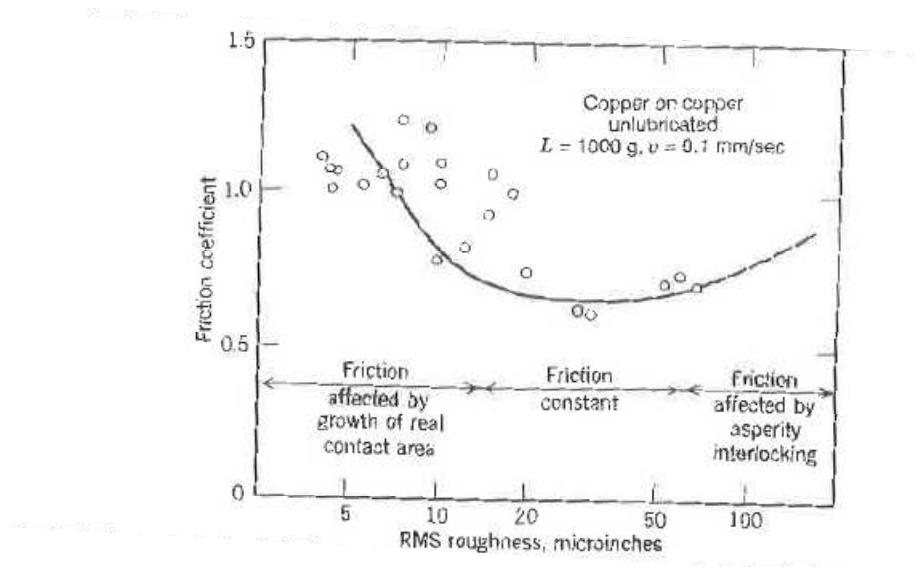


Figure 2.1 - Plot of friction against roughness shows a negative slope region caused by excessive junction growth, and a positive region caused by interlocking of asperities. In between, friction is independent of roughness. (After Ref. [17])

2.3.2. Asperity Based Friction Modeling

Examining the causality between asperities and friction in metalworking is another area where a number of studies have been performed. In a study conducted by Leu [19], a model was proposed for calculating the coefficient of friction that incorporated asperity deformation and direction of contact to account for frictional effects. The researcher focused on previously published dry, cold forming experiments, and compared their model against the existing data. The model was separated into two parts; one for asperity contact and deformation, and a second for sliding and shearing of asperities. By assuming that the asperities were cantilever beams with equal constant cross sections, Leu tried to predict the coefficient of friction, stress, and loads needed to deform specimens based on an asperity density value. The density value was directly tied

to the surface roughness measurement in two directions on the die surface. Leu attempted to account for asperities density differences when calculating forces and what the observed coefficient of friction would be based on the surface roughness. He found relatively good agreements based on the previous data, but the microscopic scale level and lack of information regarding asperity distribution on a die surface, limits the usefulness of the model for analyzing bulk flow conditions. The study did make a good attempt at combining the factors of sliding friction, directionality of the asperities, and the deformation of the asperities into a cohesive model.

Mahrenholtz, Bontcheva, and Iankov [20] also attempted to create a friction model based on asperity interactions at the die and work piece interface. The model assumed a fixed asperity distribution for a given roughness value. Asperities on the work piece surface were modeled as conical points assuming that the coefficient of friction is anisotropic (i.e. there are different values of friction in different flow direction). A finite element analysis program was used to model a very small section of the tool (on the scale of $11\mu\text{m}$), and different asperity heights and distributions were run to fixed die displacements. They simulated a normal downward force, which then caused the work piece to spread outward, causing asperity sliding as well. The coefficient of friction was then determined by examining the plastic deformation of the asperities, as compared against the normal deformation to be expected when forming. The researchers called this expected deformation the “normal compliance law” which was determined empirically using material constants. The experiment overall showed that the coefficient of friction did have a dependence on the asperity density and height. Additionally the asperity deformation had a dependence on the directionality of the coefficient of friction and had a

positive proportional relationship. However, due to the micro-scale of the model and its complexity, application of this work to study bulk flow on a macroscopic surface using roughness is not feasible.

2.3.2.1. Asperities and Lubricant Interaction

Dubar and others [21] completed similar work to that done by Mahrenholtz et al, examining lubrication mechanics at the meso-scale for cold aluminum strip drawing. This study examined the way the fluid pressure of a liquid lubricant affects deformation of asperities and lubricant pockets on a die surface. An FEA package was used to model the fluid interactions with asperities. The researchers point out that in the actual test, the coefficient of friction is unique for each side of the die used for the drawing operation. However, the resulting deformation could only be used to calculate a global average coefficient of friction. The researchers conducted a laboratory experiment to verify results, but since it related to strip drawing, its direct application to forging is difficult. Both processes involve higher pressures and plastic deformation, but forging results in less material constraint, meaning that flow can change in direction numerous times before the operation is complete. In strip drawing, deformation is fixed at all points by the die but it is uniform and in the same direction. This difference means that the interaction between work piece and die is more complex in forging where flow is not fully constrained throughout the entire processes. However, the study did show that show that friction effects at each die surface is different and that current FEA techniques are not equipped to deal with a changing friction factor over the area of deformation. Instead, all

friction factor values are assumed to be an average of both surfaces, and this applies to forging as well.

2.4. Surface Roughness and the Relationship to Friction Models

Becker et al. [22] conducted a study that had both an experimental and FEA component where they attempted to use the surface roughness of a die to estimate the friction factor in cold forming. Surface roughness is normally measured with a profilometer and provides a measurement that averages asperity height over a fixed length. The researchers assumed a constant amplitude and period of a sinusoidal waveform to create an average roughness which can be compared to a profilometer measurement. Using various amplitudes and periods, the researchers calculated various die surface roughnesses. A two-dimensional finite element model was then used calculate friction factor based on the sinusoidal waveform die texture. The calculated values were then verified experimentally using aluminum rings having a 6:3:2 ratio. The ring tests were performed at room temperature under dry conditions using dies with various surface roughnesses. The surface roughnesses were measured before the test and used within the model. The deformed ring dimensions were then compared to the calibration curves to obtain a friction factor. The model to predict the friction factor based on the surface roughness closely followed the experimentally determined value. As friction factor was increased by way of increasing the amplitude or period of the sinusoidal approximation, the resulting ring inner diameter had decreased in size, indicating the friction factor had increased. A downside to this model is that each friction factor has multiple amplitude

and period combinations, which implies that one value would have to be fixed or known before the equation can be used. This correlation suggests that by taking direct surface roughness measurements, it is possible to obtain an estimate of friction factor, assuming dry conditions. However, the model does not consider the directionality of the roughness or temperature effects on metal flow.

2.4.1. Surface Roughness and its Orientation with respect to the Work piece

Menezes et al. [23] studied the interaction between surface roughness, lay, and orientation and their effect on the coefficient of friction using metal specimens and a pin on disk apparatus. While the pin on disk test provides a convenient means to measure the coefficient of friction, caution must be exercised when applying the results to bulk deformation processes as the normal pressures employed tend to be low in comparison to the values encountered in forging. What made this study unique was the fact that the disks were ground at different angles such that the pin moved across the same roughness value but in directions that were parallel, 45-degree, and 90-degree angles to the direction of grinding (i.e. lay). Testing was done with and without lubricant using magnesium, aluminum, and aluminum-magnesium alloy pins on steel disks. They found that for a fixed surface roughness, the coefficient of friction increased as the angle with respect to the grinding direction increased. These results support the hypothesis in the current study, but due to the load and deformation limitations stated above, these results need to be verified under temperatures and pressures that are consistent with hot forging conditions.

In a companion study, Menezes et al. [24] used the same pin on disk test and increased the number of surface roughnesses used for the steel plates, but kept the same grinding directions. This time they used pure aluminum pins that were roughened using either emery papers or polishing wheels using various buffing powders. By following the same procedure, it was concluded that surface texture, which was the direction the disks were roughened, was more important to the coefficient of friction than the overall surface roughness even over a range of 30 μin to 1 μin . The results further strengthened the companion study that also concluded that part and die lay with respect to surface was important to friction. However, the study was conducted at room temperature and utilized very smooth surfaces for the steel plates (in the range of 1-10 μin) that are not typically used for forging dies.

Bay and others completed work with the objective to develop a more complete frictional model for use in finite element process analysis. The researchers wanted to develop a test that better reflects the effect of friction on the flow mechanics at work in a forging processes, due to the higher pressures used. Additionally most simulations use friction models that do not take into account all factors that can influence friction. An improvement to these models would increase the accuracy of metal flow and tool stress calculations, especially in multiple step processes. By better understanding the frictional mechanics at work in multiple step experiments and processes, more complete equations and factors within them can be added to reflect the true process, leading to improved accuracy of the model. A combination friction factor test was developed based on combined upsetting and forward extrusion coupled with a rotation of the die against a work piece. The test can be completed with an open or closed die geometry, depending

on the die and work piece pressures that are desired for the test. The basis for the test is that upsetting using a constant load is performed and is followed by rotation of the upper die. To determine the friction factor, the torque needed to twist the die was measured, while holding vertical force constant. The torque is a result of the friction factor since it is defined by the amount of force needed to shear the material. This accounts for flow occurring in both the radial and hoop directions of a specimen. Earlier experiments also completed by Bay [25] were able to determine that in this test apparatus, the bulging of the specimen was minor, and varied little with an increase in friction factor. The experiment ran aluminum, low carbon steel, and stainless steel cold in the open and closed die test apparatus, and was completed with and without lubricant. The tools were also preheated to 25 °C, 110°C, and 190 °C in order to minimize cyclic heat loads experienced by the dies while completing the cold forming operation. Bay and co-workers [25] observed that the tool temperature had a large effect on the frictional factor, while the overall sliding length and speed, caused by the twisting, had a very minor effect. Their results suggest that sliding length and speed represent minor effects, in comparison to tool temperature, which is highly influential on friction in a forging process.

2.5. Friction Relationships Found in Other Bulk Deformation Processes

Forging is considered to be a bulk deformation process and as such, other insights into the interaction between friction, die or tool roughness, and directionally can be found in other bulk processes. For example, rolling and drawing processes involve steady state

deformation but also result in large deformations and are highly dependent on frictional effects. Additionally, steady state processes such as drawing and rolling tend to employ higher sliding speeds when compared to non-steady state processes, which includes closed die forging.

Rasp and Wichern [26] studied flat drawing, rolling, and plain strain upsetting to analyze surface roughness and lay with respect to friction factor using aluminum work pieces on dies. Their study focused on asymmetric friction upsetting which uses plane strain deformation to simulate conditions occurring in a roll gap.

To clarify, asymmetric refers to the frictional conditions at each platen and means that the friction factor is substantially different between the two. Asymmetric friction upsetting uses a piece of sheet metal on a die set that has narrow platens which are compressed using a hydraulic press to a known true strain value. The sheet metal overhangs the dies on either end and after the compression takes place, the specimen bends at both ends of the setup. The specimen side that has the higher friction will have a greater angle. The resulting bend angles are measured and are directly related to the friction factor, utilizing a model that based on a frictionless operation.

Unlike the other studies reviewed in this chapter, the surface of the aluminum work piece was roughened on opposite faces by different processes that included polishing, chemical etching, and grinding with emery paper. Upsetting was varied parallel and perpendicular to the direction of the long axis of the aluminum, producing a texture i.e. lay that could be orientated to the dies. The test was run at room temperature both with and without lubricant. Based on the results from the study, Rasp and Wichern concluded that having the lay perpendicular to the rolling direction helped reduce friction

factor when using lubricant. However, no correlation was found between friction factor and the work piece lay. While the study shows promise in drawing a relationship between part lay and texture, it was done to simulate rolling and drawing and has a limited application in the world of forging, where the asperity strength of the tool is much greater than that of the work piece. In cold forming, the asperity yield strengths are much closer to each other.

Stahlmann and his co-workers [27] used FEA simulation to investigate how friction factor in a wire drawing process changes the resulting surface topography of the drawn part. The investigation focused on a multi-stand cold drawing process and the evolution of the surface roughness of a wire as it was reduced using a series of progressively smaller dies. The researchers broke down each drawing stand into multiple steps which were modeled in an FEA simulation. They broke down the process in order to capture as much of the physical mechanics at work and to increase the model resolution. The primary variables that were varied included contact normal pressures, die angles, and lubricant properties. A separate calculation block outside of the main FEA solver was used that increased the number of elements on the surface nodes. The solver then proceeded with calculations based on the increased resolution to further the accuracy of the nodes on the surface and their respective deformation based on the variables listed above. The resolved nodes were then reintroduced to the FEA solver, the model re-meshed, and the calculation cycled until the error was acceptable. The calculation cycle was then tested against a manganese-chromium alloy slug in a barrel-compression-and-sliding test where a cylindrical specimen was forced through a die at various fixed loads. The resulting geometry was then used to examine friction of the die. Overall, the FEA

methodology produced good correlation to the actual data. While the study was not a true forging application and completed a room temperature, it is still a very close approximation since both utilize high pressures and deformation. However, even though forging results in more material movement, the fact that an FEA model could be adapted to add increase resolution of surface topography on a die, shows promise for forging FEA applications.

Lastly, research conducted by Behrens [28] sought to develop a FEA based program to predict die wear in hot forging applications. Starting from Archard's wear equation, the researchers discretized the equation based on forging speeds, die material properties, and temperature that was used in conjunction with stress data from a FEA model used for forging. The researchers then compared resulting wear prediction calculations from the modified Archard equation for dies used in industry and calibrated the equation by using a wear coefficient factor. This factor takes into account surface roughness and friction within the die that causes accelerated wear. The decrease in the number of asperities usually associated with an increase in surface roughness causes more die material to deform and eventually wear. After calibration, the researchers were able to reliably predict where a die would first wear and how deep the wear track would be. The model only helped to determine the proper die material that should be used, as well the length of time between die servicing. However, if the concepts gained in the present study are applied to this type of die wear analysis, a more accurate and complete analysis could be completed. Additionally, the number of calibration runs needed could also be decreased, based on this model improvement. The promise from the study is the

combination of a FEA package and wear estimation, which will be very useful in the future of the forging die design and optimization.

3. Experimental Setup

3.1. Press Setup & Die Tooling

The experimental apparatus used in the study to conduct the forming tests consisted of a Technovate 10-ton hydraulic press (Technovate Inc., Pompano Beach, FL) that had a three-inch stroke capability. An instrumented die set that was designed and built by a team of engineering students at Marquette University as a part of their Capstone Design Project was mounted on the press frame. Two circular AISI H-13 platens were attached on a four post Superior Die Set (Superior Corp., Oak Creek, WI) and a pair of 100 W Incoloy sheathed 0.25” outer diameter cartridge style resistive heating elements (Omega HDC08691, Omega Engineering, Stamford, CT) were embedded internally and used to heat the platens to the desired temperature. One-inch thick granite backing plates were used as a barrier to minimize thermal conduction from the platens to the press and instruments. This set up has been used in previous hot forging studies at Marquette University with good success and enables die heat up rates of 10 minutes or less. Figure 3.1 and Figure 3.2, respectively, show photographs of the press and die setup that was used in the study.

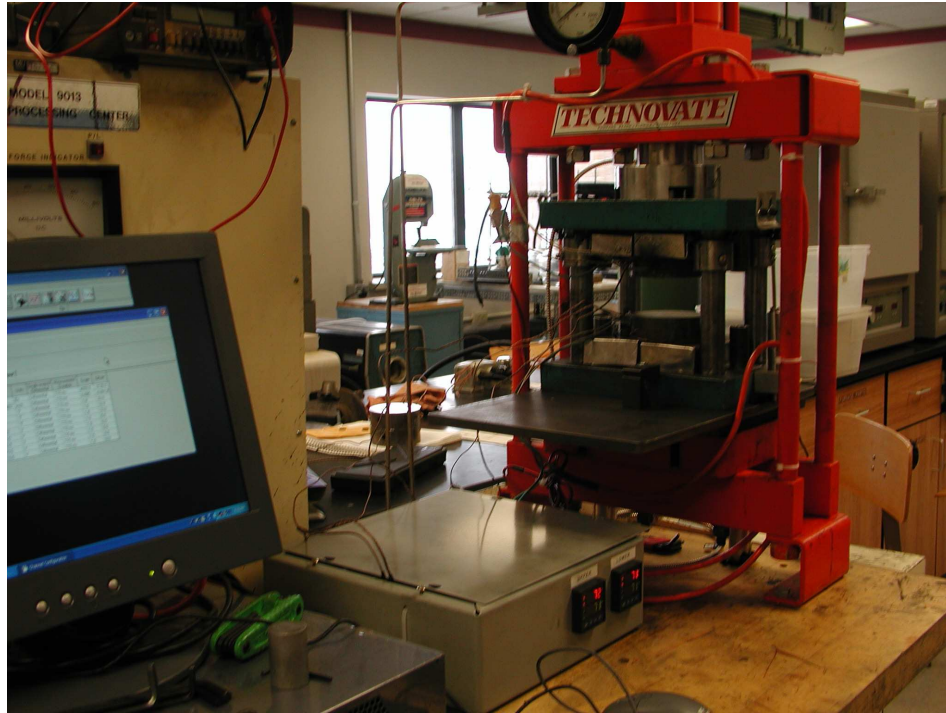


Figure 3.1 - Photo showing the Technovate press with die set, data acquisition, and temperature controllers mounted.

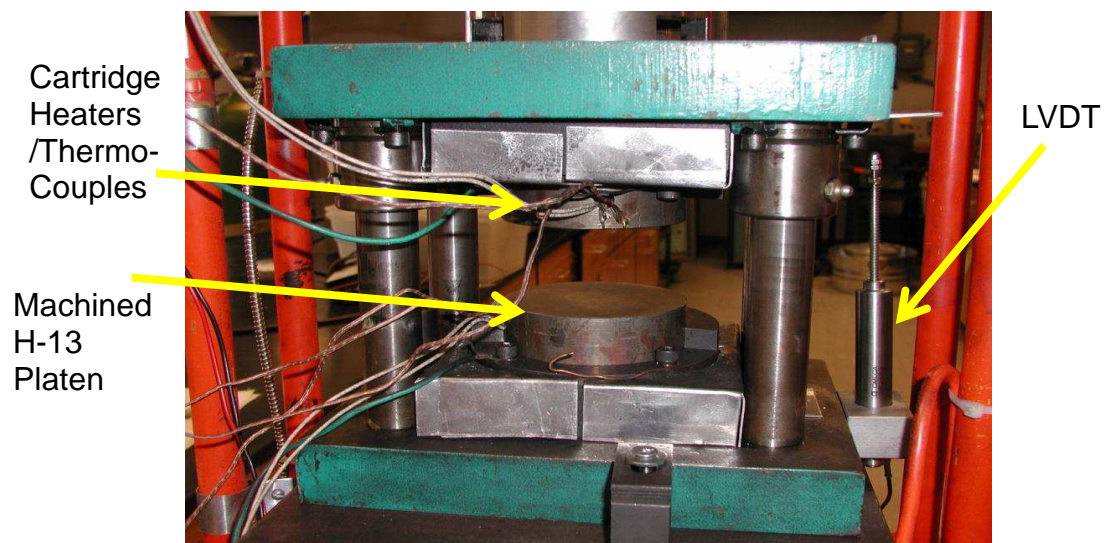


Figure 3.2 - Close up view of the experimental die setup used in the investigation with key parts labeled.

The die set was instrumented with a Helm Instrument load cell (Helm HCS05-10T, Helm Instrument Co., Maumee, CT) to measure forming loads and a linear variable differential transformer (LVDT) to record die position as a function of press stroke. Two independent sets of K-type sheathed thermocouples were mounted on the edge of the working surface of each platen. One set was used to provide feedback for the temperature control units while the second enabled data logging of the die surface temperature. Temperature control for each platen was achieved by a feedback loop using a set of thermocouples and a proportional integrative derivative (PID) controller. This enabled surface temperature of both platens to be individually controlled and maintained to within $\pm 4^{\circ}\text{F}$. The K-type thermocouples used within the control system were accurate to $\pm 1^{\circ}\text{F}$. All measurement devices were connected to an iOtech Data Acquisition (Personal Daq/54, Measurement Computing Corporation, Norton, MA) system so that the data could be electronically recorded using pDAQ software and stored on a desktop computer that was connected via USB. The pDAQ used in conjunction with the desktop enabled one data point to be recorded every second. Figure 3.3 shows block diagram of the press system and instrumentation setup.

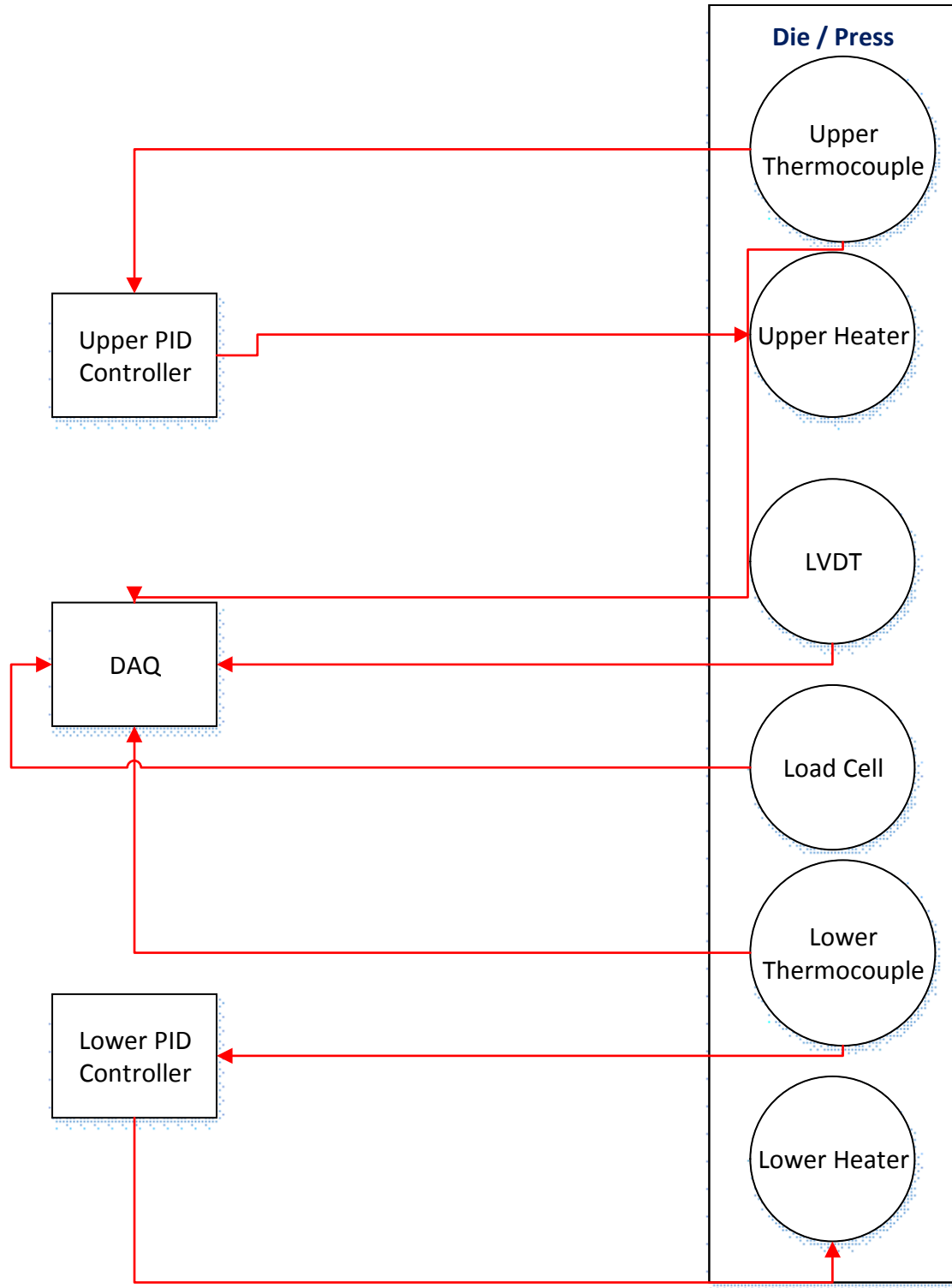


Figure 3.3 - Block diagram of instrumentation and PID controllers used on the hydraulic press and die set.

Three different types of experimental tests were conducted as a part of the study: a.) cylindrical upsetting to correlate die temperature to the observed friction factor, b.) cigar testing to examine the effects of part orientation with respect to the die roughness and lay, and c.) ring testing to provide an average measure of friction factor for each die roughness that was used. Each test and the procedures used are described separately in the sections below. A description of how the die platens were machined to achieve the desired roughness and lay for each test is presented in the following section. All dies were heat treated to a hardness of 50-55 on the Rockwell C scale prior to testing.

3.2. Die Machining Procedure Used to Achieve Controlled Surface Topography

To achieve a controlled surface lay and roughness for the compression tools employed in each experiment, one inch thick, four-inch diameter AISI H-13 platens having oriented grooves were used. H-13 tool steel was the platen stock as it is widely used as a hot forging die material due to its hardenability, hot hardness, and fatigue resistance.

A majority of the tests were performed without any lubricant, i.e. “dry”, for the following reason. While lubricants have a significant effect on friction, their application on a die surface is very difficult to control to a level that is needed to produce repeatable results for a research study. A key challenge is ensuring that a consistent, even layer of lubricant is applied, and this often requires use of a precisely metered system capable of atomizing the spray. Nevertheless, since lubricant is widely used in forging operations,

lubricant was used under selected test conditions in order to verify if the results and findings were valid under representative process conditions. Manual application was employed, but it was a challenge to ensure that excessive caking and buildup of lubricant did not occur on the die surfaces causing inconsistent deformation and data scatter.

3.2.1. Platens Used for Cigar Test

As discussed in Chapter 2, the cigar test is a method to measure the relative friction factor in a die setup. In this study, it was chosen due to the fact that it allows for material flow in two directions and can then be used to determine differential flow in a plane. To perform the cigar test, it was desired to machine the platens such that the lay was unidirectional. As a result, metal flow could then be assessed when the longitudinal axis of the work piece was orientated parallel, perpendicular, and diagonal to the primary direction of the surface lay as depicted in Figure 3.4 using a range of surface roughnesses.

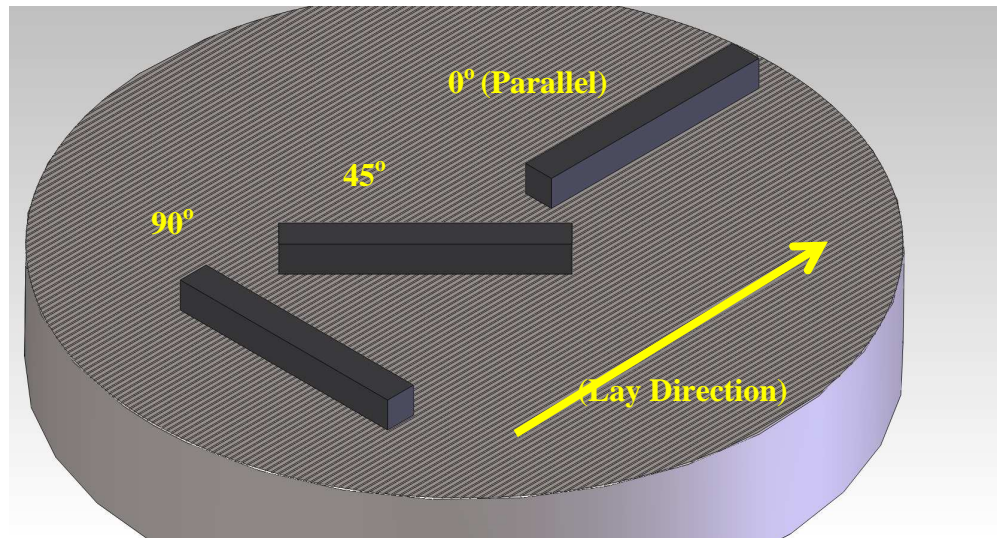


Figure 3.4 - Schematic showing different specimen orientations used to assess the effect of part lay. From left to right, the longitudinal orientations of the specimens are, 90° , 45° , and 0° (parallel) with respect to the surface roughness.

For the cigar test, surface roughness corresponding to 4, 40, 60, 125, and 250 μin in R_a were used. A standard flat grinder was used to machine platens having surface roughnesses of 4 μin , 40 μin , and 60 μin R_a . For each roughness, the grinding direction was marked on the surface of the platen after machining so that proper specimen orientation could be achieved prior to each test. For surface roughnesses greater than 60 μin , grinding could not be used and a special milling sequence had to be employed in order to achieve a consistent surface roughness and lay for the 125 and 250 μin , R_a platens. These values correspond to the higher end of roughnesses and were selected as they are representative of surfaces observed on worn forging dies. After grinding, the dies underwent heat treatment to a Rockwell C value of 50-55. The 4 and 40 μin dies were heat treated in a cracked ammonia environment in a Marquette University oven, while the

60, 125, and 250 μin dies were heat treated in an neutral environment at a local heat treatment company, ThermTech Inc of Waukesha, WI.

While end milling is widely used to machine commercial forging dies cavities, the resulting surface topography does not provide a sufficient level of lay directionality needed for investigative purposes, and this necessitated development of a special milling sequence. This was accomplished by machining parallel grooves having a constant depth on each of the platens using a HAAS TM-2 milling machine and a #2 center drill tool. All platens were milled in the annealed condition in order to facilitate machining and achieve reasonable tool life and later hardened. The top and bottom surfaces were first face milled smooth and parallel to within $\pm 0.002''$. A second pass was then performed using a #2 center drill rotating at 4000 rpm and set to a 0.0001'' depth of cut. The actual depth of cut was closer to 0.004'' due to manufacturing variations. Figure 3.5 shows a close up view of the representative marks on one of the 125 μin R_a platens after machining was performed on the HAAS mill.



Figure 3.5 - Close up view of the grooves on the 125 μm R_a die after machining. The magnification is 400x.

For the 125 and 250 μm platens, consistent lay directionally was achieved by performing parallel linear cuts in one direction over the surface. The pitch or spacing at which the center drill was offset after each cutting pass was then varied to achieve the desired surface roughness. Using repeated passes at various pitches; it was possible to create a consistent lay direction and uniform surface roughness. See Figure 3.6 and Figure 3.7 for a schematic of the die surface for the 125 and 250 μm roughnesses and their respective pitches. After machining, the dies were heat treated to a Rockwell C of 50-55 at Thermtech Inc, a heat treatment company in Waukesha, WI using a neutral atmosphere.

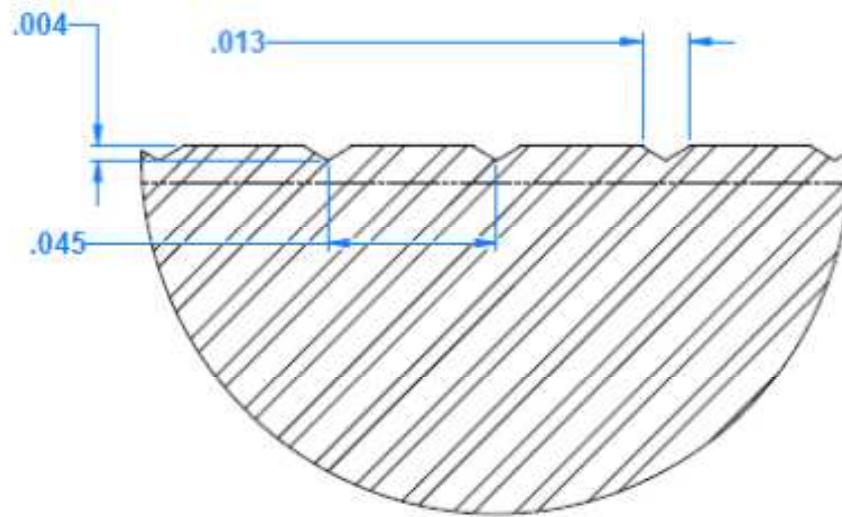


Figure 3.6 - A schematic of the 125 μm R_a platen surface after machining. All dimensions are in inches.

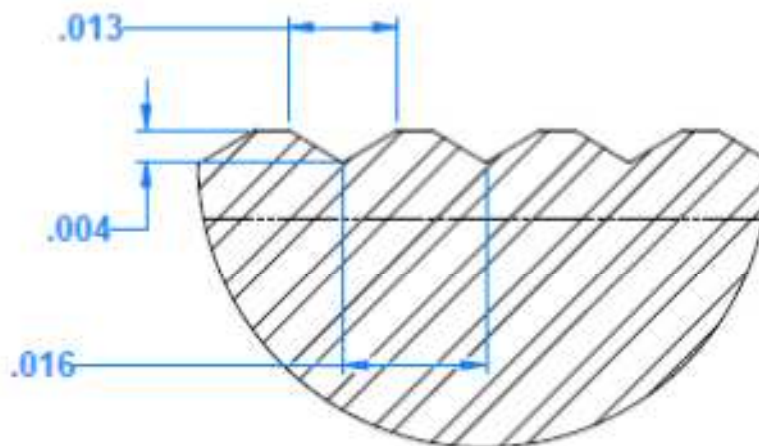


Figure 3.7 - A schematic of the 250 μm R_a platen surface after machining. All dimensions are in inches.

3.2.2. Platen Machining Used for Cylindrical Upset Testing

In order to quantify the effect of temperature on friction factor and observed deformation, the ring test and a cylindrical upsetting test were used. The ring test provided a direct means to measure the friction factor while the cylindrical upsetting test provided a way to see the frictional constraints on a larger part.

As the ring and cylindrical upsetting tests involve both radial flow, it was desired to use machining marks that were perpendicular to the primary flow direction of the specimen. Figure 3.8 depicts a top view of a ring specimen on the die and the flow directions of the outer and inner diameters. Consequently, a Computer Numerical Controlled (CNC) lathe was used to face the surfaces of the platens. This enabled concentric circular lay marks to be machined on the platens and allowed radial flow to be perpendicular at all points on the cylinder and ring specimens. Each platen was made of H-13 and was turned after heat treatment to achieve an average surface roughness of R_a 20 μin so that friction factor could be determined as a function of temperature. Roughness values for all platens were checked after machining using a Federal Esterline profilometer.

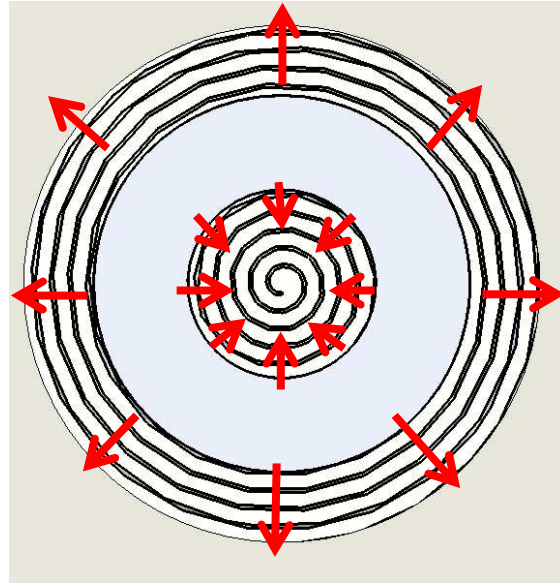


Figure 3.8 - A schematic of a ring test specimen on the machined die platen with concentric lay. The arrows indicate the direction that the point will flow. Note how the arrows intersect the machined pattern at perpendicular angles.

3.3. Work Piece Material and Geometry

The work piece material used in all the tests was 6061-T6 aluminum bar stock and was chosen due to furnace temperature and press load considerations. The work piece geometries that were chosen for the study included: 1.25" diameter x 1.125" high cylinders, 0.25" square x 2" long bar, and 1.125" outer diameter by 0.5625" inner diameter by 0.375" height rings (i.e. 6:3:2 ratio). Cylindrical specimens were used to examine the effects of different die temperatures on friction factor while the rectangular specimens were used to investigate the effect of part lay and roughness on flow. Ring specimens were used to acquire an average value of friction factor on the die surface at each roughness for comparison purposes on each of the linear lay surfaces. All work piece lengths and flatness were machined to within ± 0.002 " and each specimen

underwent a two-part vibratory bowl treatment prior to testing to ensure a randomized and uniform surface finish of R_a 35 μin . Figure 3.9 shows the representative surface of each work piece geometry after vibratory finishing was completed.

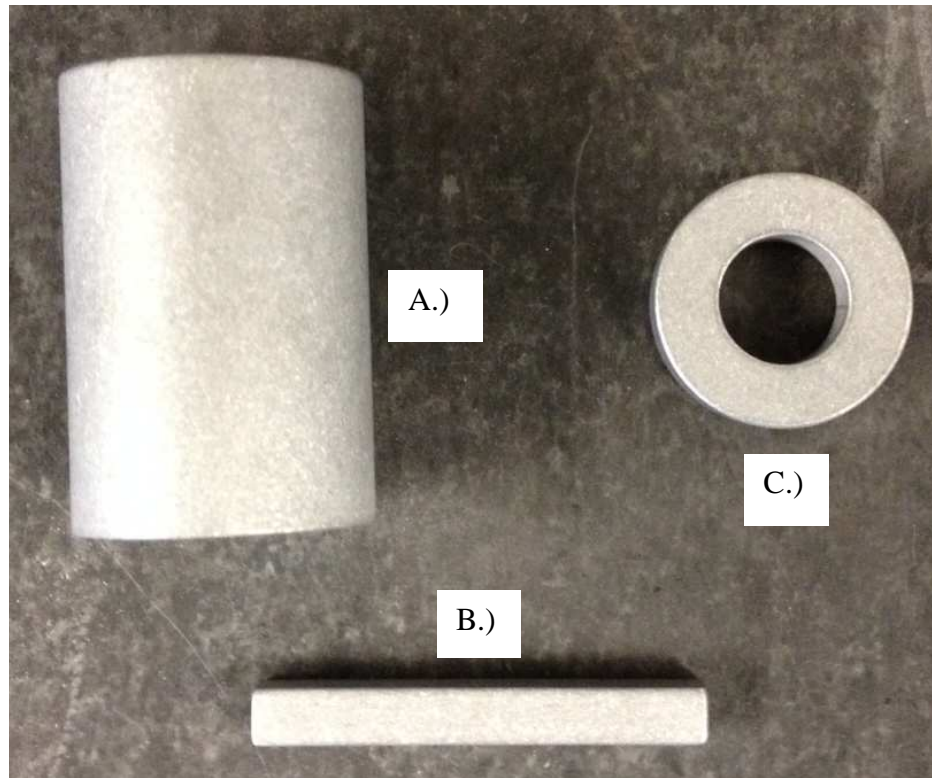


Figure 3.9 - A display of the various aluminum specimens used in the study. From left to right: A.) cylindrical specimen B.) rectangular specimen and C.) ring compression test specimen.

3.4. Summary of Experimental Methodologies

3.4.1. Cylindrical Upsetting Test Methodology

As friction is directly related to the amount of curvature present on the sides of a deformed cylindrical work piece, 1.25" diameter specimens were upset on the 20 μin R_a die with concentric lay. This enabled the effect of die temperature on the friction factor to

be analyzed based on the resulting bulge radius without having lay confounded into the experimental results. Due to the fact that surface temperatures are not static during forging due to the effect of die chilling, four different die temperatures (250, 300, 350, and 400°F) which were consistent with those observed in a commercial closed die forging process were used. The aluminum specimens were heated to 826°F using a Lindberg box-type resistance-heating furnace and held for two hours prior to testing to ensure a uniform work piece temperature. 826°F was chosen as the hot working temperature, as it represents the average range of temperatures used for various aluminum alloys.

Each cylindrical specimen was upset to a true strain of 0.7 after which the bulge/barreled profile of the as-forged geometry was measured on a Browne & Sharp coordinate measuring machine to determine the bulge radius. Figure 3.10 shows a representative cylindrical specimen after compression, and the bulged sides are clearly evident. Table 1 below shows a summary of the test conditions and geometry used. For each test condition, five replications were performed.

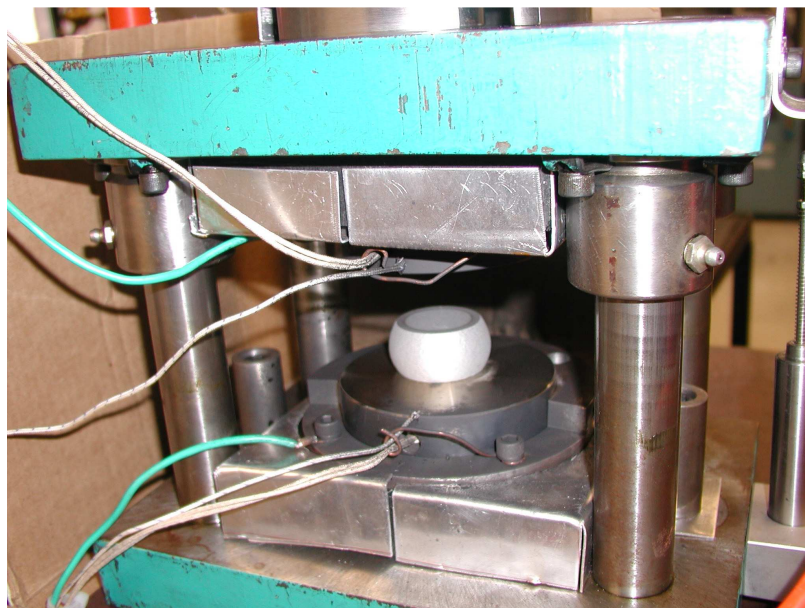


Figure 3.10 - A cylindrical specimen shown after compression. Note the bulged sides.

Table 1 - Summary of conditions used for a portion of the temperature study. The test consisted of cylindrical specimens upset at the listed temperatures and the resulting bulge radius measured. Note that this test was completed without lubricant.

Part Geometry	Die Temperature (°F)	Die Roughness (μin)
OD:H 1.25" x 1.875"	250 300 350 400	20 μin

3.4.2. Cigar Test Methodology

In order to investigate the effect of surface roughness and lay on metal flow the cigar test was used. For each surface roughness, the longitudinal axis of the 0.25" square specimens were orientated at angles of 0°, 45°, and 90° with respect to the direction of the machining/grinding marks on the die surface. An alignment tool was developed and used to ensure the specimens were aligned to within $\pm 5^\circ$ of the desired orientation (0°, 45°, 90°) prior to compression. By mounting a laser pointer on a magnetic switch base and using a plastic protractor aligned with the machining marks on the die surface, notations were made on the steel base plate where 45° and 90° would align with the laser pointer. After being aligned, each specimen was then compressed perpendicular to the longitudinal axis using the hydraulic press and H-13 platens at roughness values ranging from 4-250 μin while holding the die temperature constant at 400°F.

In all runs the specimen was compressed until the press stalled which resulted in an upset strain close to 0.7. After cooling, the length and width of the compressed bar specimens were measured using a dial caliper. Due to non-uniformity of metal flow in the

vicinity of the corners; height, length and width, were measured at the mid-point of each specimen as shown in Figure 3.11. Specimens were run with and without lubricant.

Dylon FW-3629, which is a graphite colloid, was used as the lubricant and was diluted to achieve a 30:1 ratio of water to graphite. The lubricant was applied to the working surface of each platen using a spray apparatus which consisted of a single 120° full cone nozzle and a 150 PSIG pressurized canister. The dies were separated to the maximum standoff of the press, and the lubricant applied for a two second interval on each platen prior to compression. Die surface roughnesses were periodically monitored using a profilometer to ensure that die wear did not have an adverse effect on the experimental results. Table 2 below shows a summary of the conditions used for the cigar tests. At each test condition, five replications were performed.

Table 2 - Summary of conditions used for cigar testing. The test investigated material flow with respect to part lay and was completed and without lubricant.

Part Geometry	Die Temperature (°F)	Part Lay	Die Roughness (μin)
0.25" x .025" x 2"	400	0°	4
		45°	40
		90°	60
			125
			250

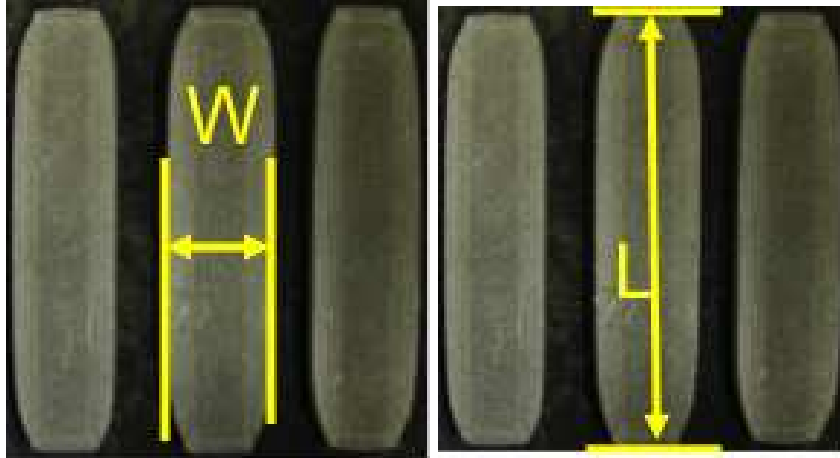


Figure 3.11 - Plane views of representative forged prismatic specimens with the width and length dimension, w and l respectively, indicated. The orientation of each specimen is discernible from the lines on the surface of each specimen.

3.4.3. Ring Compression Test Methodology

The ring compression test was conducted for each temperature and surface roughness, using dry and lubricated surfaces, to obtain an average friction factor value for each die platen. Rings having a ratio 6:3:2 (OD:ID: Height) were machined from 1.125" diameter aluminum bar stock. A 6:3:2 ratio was selected for the study since it minimizes the strain rate sensitivity of the aluminum as reported by Dutton et al. [6], who found that it resulted in a balance between measurable deformation and friction factor variations caused by a material's strain rate sensitivity. Determination of the friction factor was performed using the method outlined by Male and DePierre and consisted of measuring the deformed inner diameter and height using dial calipers and comparing the ratio to a standard calibration curve. Table 3 and Table 4 below show a summary of the conditions used for the ring compression test.

Table 3 - Summary of conditions used for a portion of the temperature study. Ring specimens were upset at the listed temperatures and the resulting friction factor measured. No lubricant was used for this portion of the test. These tests are represented schematically in Figure 3.8

Part Geometry	Die Temperature (°F)	Die Roughness (μin)
OD:ID:H 1.25":0.625": 0.417"	250	20
	300	
	350	
	400	

Table 4 - Summary of experimental conditions used to study the effect of surface roughness on friction factor. Ring specimens were upset on dies which had the listed surface roughness values while the temperature was held constant. Tests were performed with and without lubricant. These tests are represented schematically in Figure 3.12

Part Geometry	Die Temperature (°F)	Die Roughness (μin)
OD:ID:H 1.125":0.563": 0.375"	400	4
		40
		60
		125
		250

Table 3 focuses on the effect of temperature on friction factor, while Table 4 only deals with the part lay and orientation variables. Since Table 3 involves only temperature variation, the 20 $\mu\text{in } R_a$ concentric die was used to complete the test. A schematic of material flow for this test is presented back in Figure 3.8. The ring tests completed on the linearly machined dies are presented schematically in Figure 3.12. At each test condition, five replications were performed.

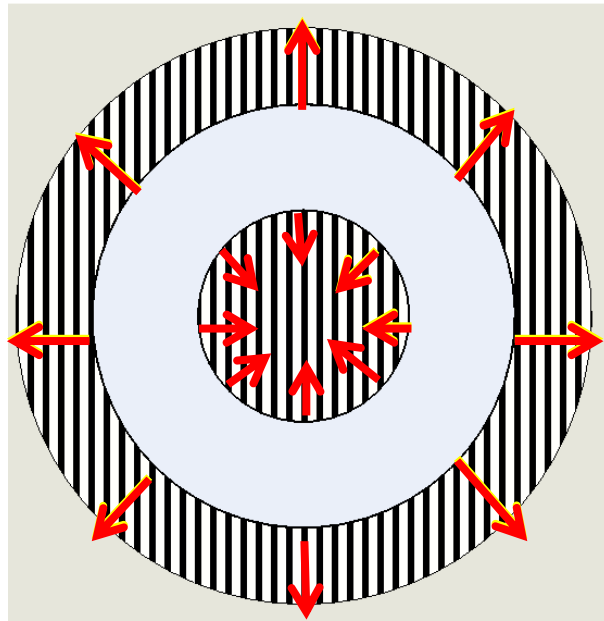


Figure 3.12 - A schematic of a ring test specimen on the machined die platen with directional lay. The arrows indicate direction that the point will flow. Note how the arrows intersect the machined pattern at angles varying from 0 to 90 degrees.

4. Discussion & Results

In this investigation, two tribological phenomena were of interest and included assessing a) the effect of die temperature on friction factor and bulge radius and b) the influence of surface lay and roughness on material flow. As discussed in Chapter 3, three different compression tests were performed in order to study these phenomena and consisted of cylindrical upsetting, cigar, and ring tests. The ring and cylindrical upsetting tests were used to investigate the effect of die temperature on friction, while the cigar and ring tests were used to explore the relationship between surface topography and material flow. A finite element simulation was also conducted using the commercially available DEFORM software code to visualize local material flow in the vicinity of the die/work piece interface during the cigar test. The organization of Chapter 4 can be summarized as-follows. First the results of the cylindrical upsetting test are presented and discussed. Then results obtained from the cigar test and the ring compression tests are presented and discussed in turn.

4.1. Cylindrical Upset Testing Results

The cylindrical upsetting test was performed to examine the relationship between friction factor and die temperature which was varied from 250 °F to 400 °F in 50 degree increments. The tests were conducted using platens having a constant surface roughness of 20 μin , which is consistent with the finish on a new die surface. Figure 4.1 below shows the measured bulge radii that were obtained from compression of un-lubricated

6061-T6 aluminum cylinders which had been heated to 826°F. It can be seen from the data in Figure 4.1 that the bulge radius increased in direct proportion to the die temperature. A regression curve was fitted to the experimental data using Microsoft Excel and the resulting linear model has an R^2 value of 0.99866 which indicates that the bulge radius as a function of die temperature closely follows a linear trend. These results are consistent with those obtained by Baskaran, Arunahalam, and Narayanasamy [15] who also found that as friction factor increases, the bulge radius also increases.

At first thought, this trend appears to be counterintuitive. This is based on the consideration that as die temperature increased, it would be expected that the amount of die chilling would be reduced. Consequently, measurable friction should also be reduced since the work piece material's flow stress at the interface would also be lowered. However, as die surface temperature increases, the effect of die chilling is reduced and this allows the aluminum work piece to remain hotter over a longer period of time. It is hypothesized that the higher temperature results in an increase of the oxide layer thickness on the surfaces of the aluminum specimen, based on work published by Hunter and Fowle [29] who observed this effect in their experiments on the mechanisms of aluminum oxide formation. Normally, in a bulk deformation process using steel as the work piece, an increase in oxide formation can help to decrease friction since the flow stress of the non-oxide is weaker at hot working temperatures and the layer acts as a lubricant in flat rolling [30]. However, steel oxide formation is normally avoided in a forging process since it is very abrasive and scores the die surface. While the effect of die chilling on the flow stress of the aluminum specimen is reduced at higher die temperatures, a buildup of the thicker oxide layer on the part surface results in higher

forces needed to overcome and cause material shear. However, the relative thickness of the layer is primarily established by the oven temperature and soak time of the specimen, which were held constant in this study. Therefore the growth of an oxide layer thickness is assumed to be a minor factor in the trend in Figure 4.1.

Previous studies by Wang et al. [31] and Pujante et al. [32] have showed that in an aluminum/tool steel pair, an increase in temperature leads to an increase in adhesive wear. Adhesive wear is primarily caused by aluminum micro welding to the die surface and then adhering to other aluminum that is moving past. However, no smearing or buildup of aluminum was observed on the surfaces of the die platens that were used in the study. While not leading directly to micro welding and plowing, the increase in temperature likely increased the affinity for the tool steel and aluminum to adhere to each other. This adhesive tendency most likely overshadowed any decrease in the aluminum work piece's flow stress. However, the direct cause is not clear and warrants additional investigation.

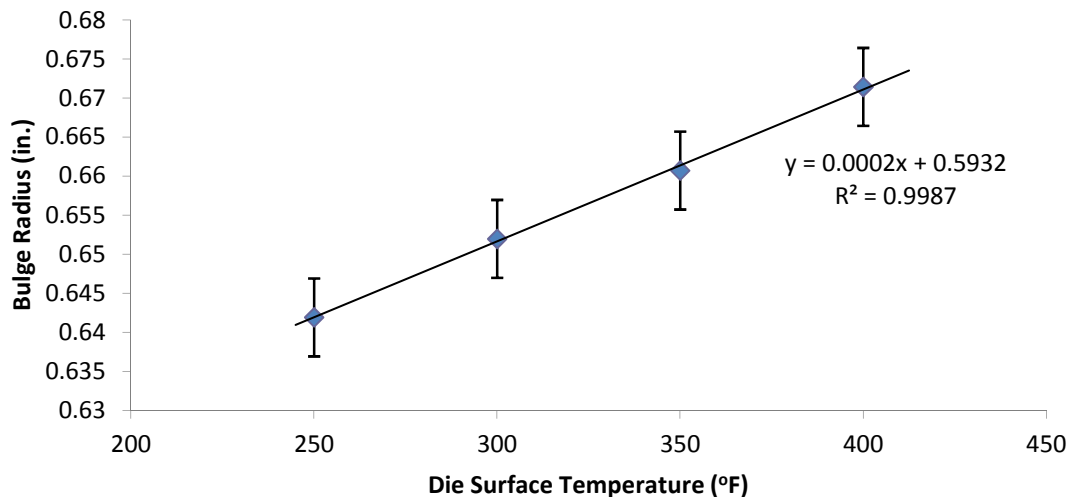


Figure 4.1 - Radius of curvature plotted as a function of die temperature for 6061-T6 cylindrical specimens

4.2. Cigar Testing Results and Discussion

As noted in Chapter 1, the cigar test was used to experimentally study the relationship between surface lay and roughness on metal flow. Since most existing frictional tests are not sensitive enough to distinguish between friction factors in two different directions, using a cigar specimen that was shorter than ten times the width was thought to provide a more appropriate means to distinguish if lay affected material flow in two orthogonal directions. This is due to the fact that flow is largely planar on a forging die surface and is comprised of two perpendicular directions (e.g. X and Y directions in a Cartesian coordinate system). The vertical flow of a work piece is governed by the press and top die movement which would represent the Z or the vertical axis. A cigar specimen in which the width is less than ten times its length will enable flow to occur in two directions in the horizontal plane. For such geometry, the maximum flow will occur on the primary direction (being the shortest) and lesser flow would be expected on the secondary direction (which is the longest), which reflects flow conditions on the surface of a forging die.

To quantify material flow or deformation, true strain is normally used in bulk forming since it can be used in increments and added together without introducing error. The true strains for the rectangular specimens in the width direction were calculated using:

$$\epsilon_w = \ln \left(\frac{w_o}{w_f} \right) \quad (4.1)$$

and similarly for the length or the longer direction:

$$\epsilon_l = \ln \left(\frac{l_o}{l_f} \right) \quad (4.2)$$

The subscript “o” represents the initial dimensions and the subscript “f” “the final dimension of the aluminum specimen. These individual strains were first considered in order to understand the fundamental effect that surface roughness and lay have on the cigar test specimen along individual axes or directions. To allow for a relative comparison or differential in flow between the primary and secondary directions, an average spread ratio was used and is defined to be:

$$S_r = \frac{\epsilon_w}{\epsilon_l} \quad (4.3)$$

Spread ratios were calculated for all conditions tested. In an actual forging die, metal height at a local region will have to get shorter due to the die travel but the material is able to pick what direction it will go in the perpendicular plane. As such, for a given die travel, an increase or decrease in one direction should result in the converse in the orthogonal direction on a horizontal plane due to constancy of volume.

What follows are the results and discussion based on individual true strain to surface roughness, then metal flow to part orientation, ending with the DEFORM analysis of localized flow at the die / work pieced interface that was completed.

4.2.1. Effect of Surface Roughness on True Strain

4.2.1.1. Un-Lubricated Tests

Presented below are the width and length strains and spread ratio obtained at different surface roughnesses for un-lubricated conditions. Due to the inherent variability in experimental data collected under hot working conditions, five replications were performed to obtain an average value. The error bars represent one sample standard deviation above and below the mean data point. Standard deviations were chosen instead of range in order to show deviation from the mean instead of maximum and minimum values. The standard deviation accounts for the number of observations that occur near a mean instead of just extreme values.

Figure 4.2 represents a comparison between die roughness and length true strain with a different data set used to represent each orientation. Figure 4.2 clearly shows that as die roughness increased, the strain in the secondary or length direction decreased. This result was to be expected since it is common knowledge that a smoother die results in better material flow up to a minimum value. After that, the increase in apparent area starts to locally bond asperities resulting in less strain. Apparent area is the actual area of contact between the die and work piece and is usually much smaller than the work piece's actual footprint due to asperity contact. A smaller R_a die surface reduces the number of large asperities the material has to move over to be able to flow, thus increasing the amount of strain.

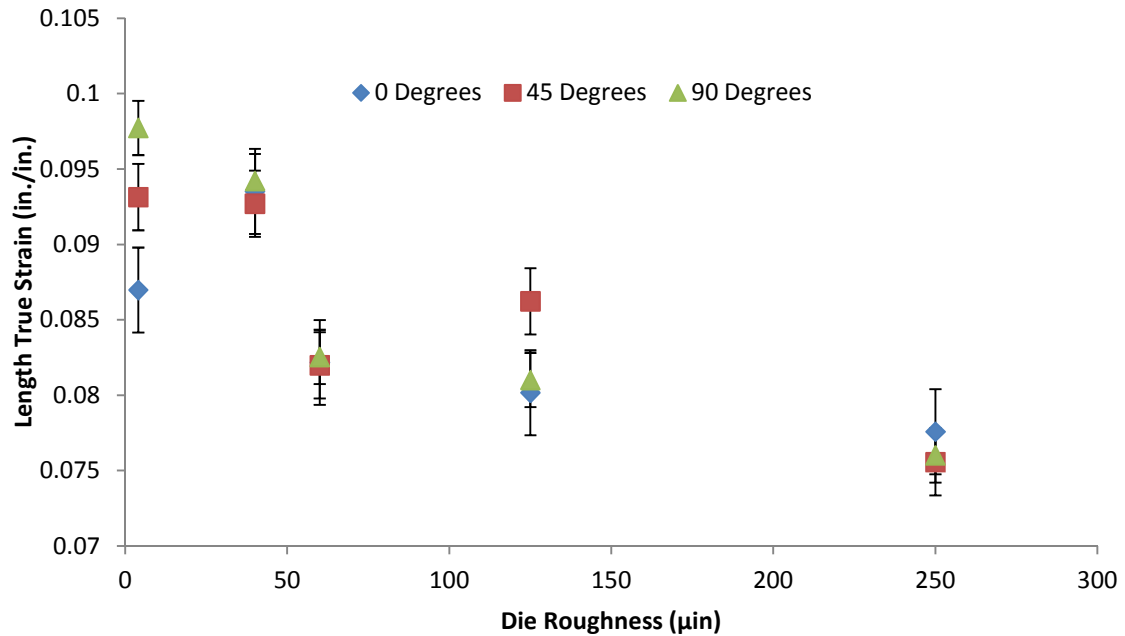


Figure 4.2 – Average length strain as a function of surface roughness for the rectangular specimens. Tests were performed without lubrication.

Figure 4.3 below plots width strain as a function of die surface roughness, again with each orientation being represented as a separate data set. Similar to the results shown in Figure 4.2, the same negative linear trend can be observed. However, the strain values in Figure 4.3 are about eight times greater than those in the secondary direction. Since the width true strain is in the primary direction of flow, the large increase in true strain is expected. No apparent shift upward or downward in true strain is caused by part orientation which is examined in the next section. Another interesting trend to observe is how Figure 4.2 and Figure 4.3 both decrease as die roughness increases. The decrease would contradict the conservation of volume, assuming that the specimen heights are the same. However, since the width and length measurements are taken at the midpoints, any bulging behavior is ignored. If there was less bulging with the same amount of overall

metal flow, both directions could conceivably decrease the midpoint measurement while still maintaining the conservation of volume. At the higher die roughness the restriction to flow is such that the material bulges less instead of flowing laterally.

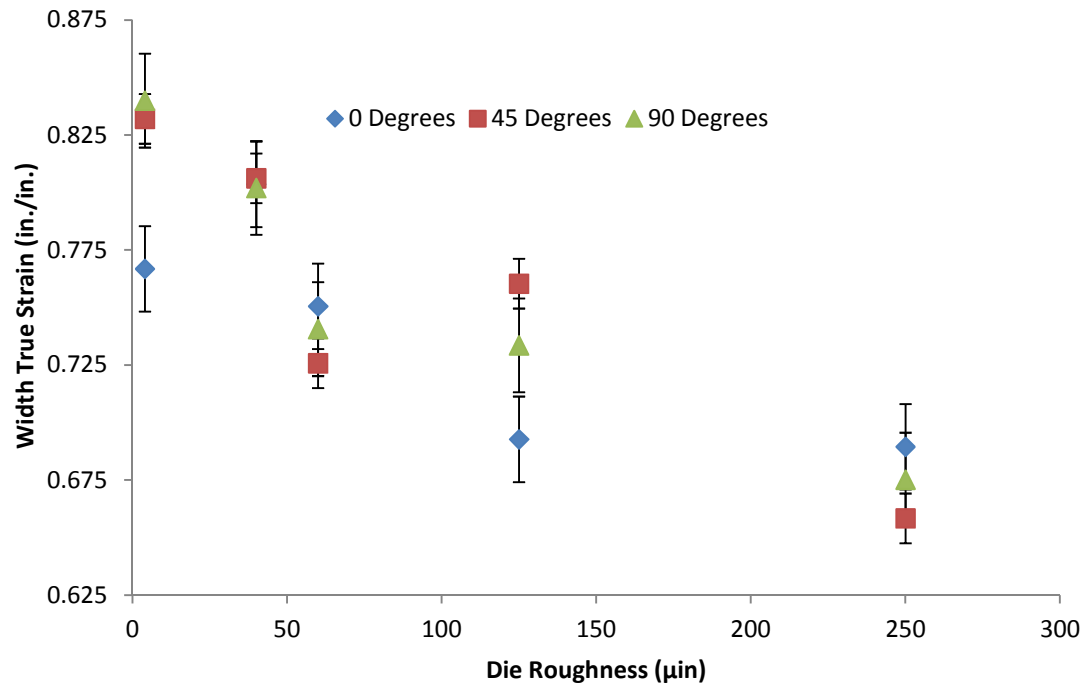


Figure 4.3 – Average width strain as a function of surface roughness for the rectangular specimens. Tests were performed without lubrication.

Figure 4.4 below shows the average spread ratio plotted as a function of die roughness, and as is the case for the preceding figures, has each part orientation represented as a different data set. The standard deviation error bars have been removed for clarity and a complete listing of all the standard deviations is provided in Appendix C. In Figure 4.4 a different trend is observed where a decrease in spread ratio occurs from 4 μin to 40 μin , after which a sudden increase is evident at 60 μin . Further increase in surface roughness then causes the spread ratio to slowly decrease again to 250 μin . There is an apparent transition area at 60 μin , which agrees with the trend shown in Figure 2.1

which was reported by Rabinowicz [17] . In Figure 2.1, the coefficient of friction linearly decreases as R_a increases from 0 to 15 μin . From 15 to 60 μin , friction remains essentially constant, and then at 60 μin a positive linear relationship develops. Around the 60 μin roughness, the material flow transitions from a growth of real contact area to more asperities colliding which results in a change in how the material flows.

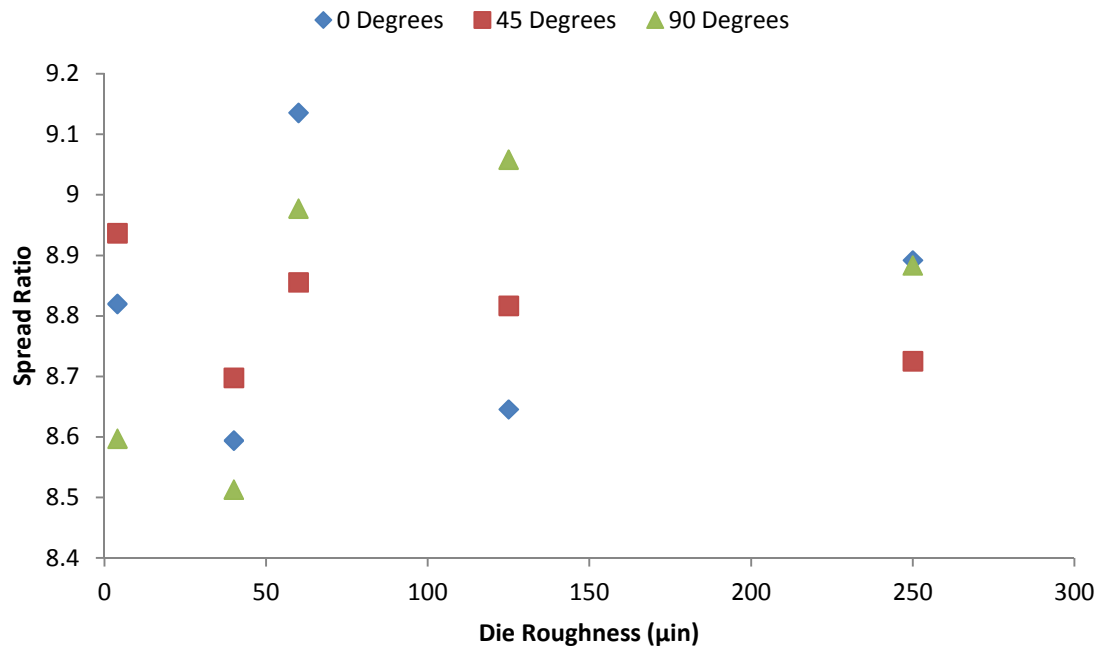


Figure 4.4 - Average spread ratio as a function of surface roughness for rectangular specimens. Tests were performed without lubrication.

4.2.1.2. With Lubricant

Below is the same data shown in Figure 4.2, Figure 4.3, and Figure 4.4 except that testing was completed using a water-based lubricant that was applied using the methodology described in section 3.4.2.

Figure 4.5 below represents a comparison between die roughness and length true strain with different data sets used to represent each part orientation. Similar to the results in Figure 4.2, a negative linear relationship is observed without any major effect resulting from varying part orientation. From Figure 4.5 it is observed that the strains at all orientations in appear to be shifted upwards by about 20% from the data in Figure 4.2.

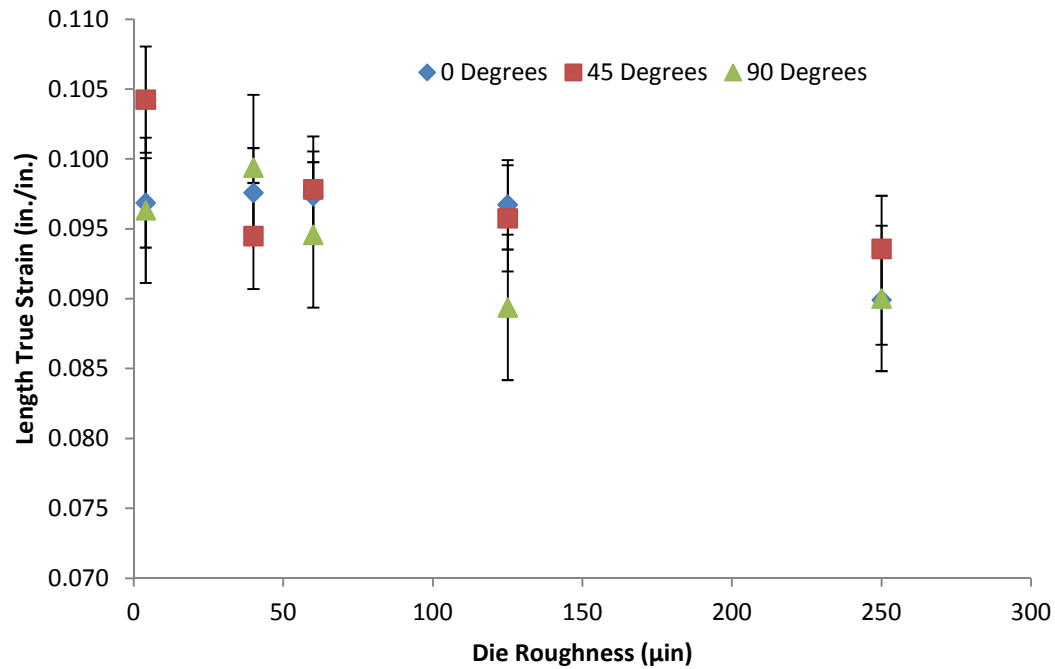


Figure 4.5 – Average length strain as a function of surface roughness for rectangular specimens. Tests were performed with lubrication.

Figure 4.6 below shows the average width stain as a function of die roughness, with the addition of lubricant. Similar to Figure 4.5, all strains were increased by about 17% due to the use of lubricant. However, the figure shows the same negative linear trend as surface roughness is increased. In this trial, the appearance of the 60 μin transition point again appears.

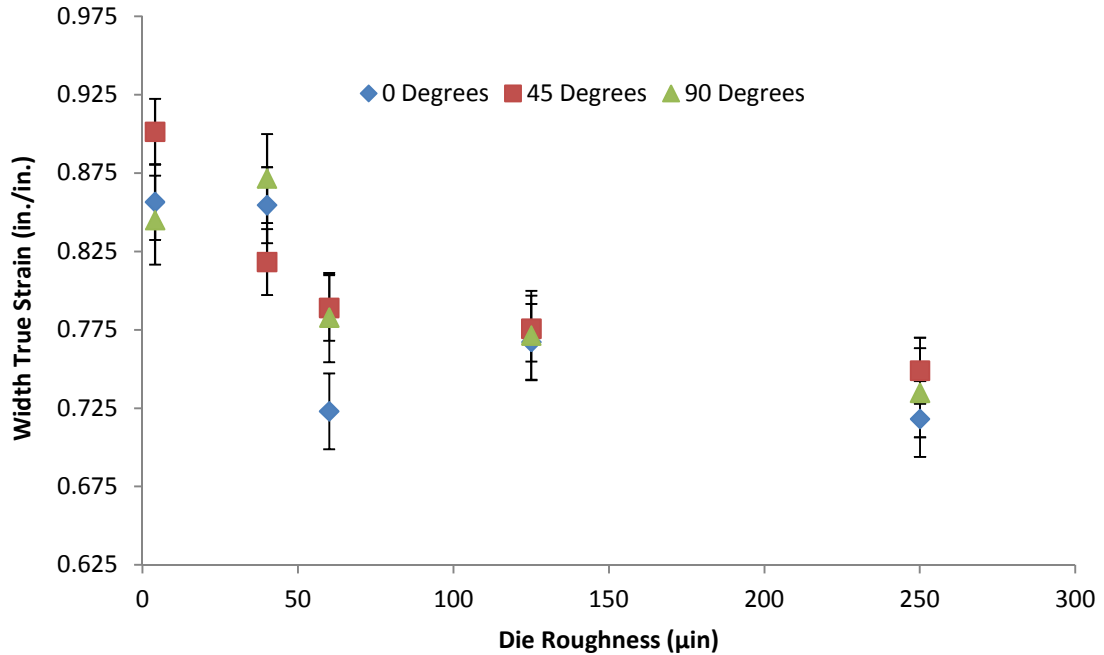


Figure 4.6 – Average width strain as a function of surface roughness for rectangular specimens. Tests were performed with lubrication.

Figure 4.7 below shows the average spread ratio plotted as a function of die roughness using lubricant. The 60 μin transition point again appears but with the use of lubricant, it represents a sudden decrease instead of an increase. The 4 μin and 40 μin dies have the same spread ratio of about 8.75 with the use of lubricant which is a slight increase compared to the value of 8.7 that was obtained from the dry results. The spread ratio actually decreased from a combined average of 8.9 for the 60 μin through 250 μin roughness to 8.1 which represents a change of about 9%. Since the spread ratio is the primary direction strain divided by the secondary direction, the decrease indicates that the primary strain increased less than the secondary strain. The lubricant allowed for more flow in the length direction, lowering the spread ratio for the rougher dies.

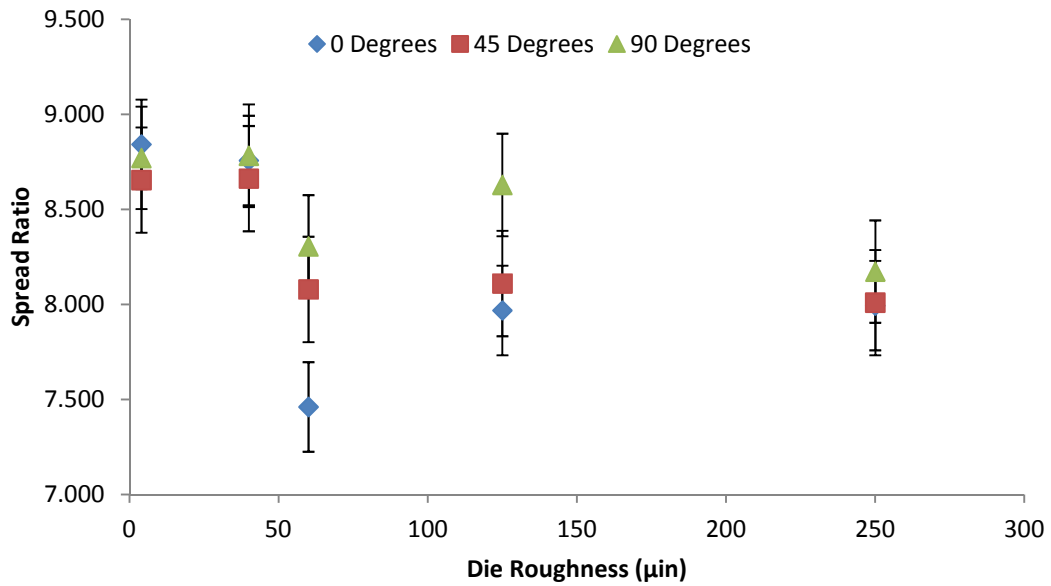


Figure 4.7 - Average spread ratio as a function of surface roughness for rectangular specimens. Tests were performed with lubrication.

4.2.2. Comparison of True Strain to Part Lay/Orientation

Below are the same results as in section 4.1, but this time comparing part orientation to average strains and spread ratio. As a result, the die roughnesses of the platens used now become the individual data sets. For clarity, each plot is broken into a rougher die and smoother die plot. Additionally, the standard deviations have been removed and placed in the table in Appendix C. Appendix A and Appendix B contain the combined plots for the dry and lubricated results, respectfully. The smoother dies are the 4 μin and 40 μin dies, while the 125 μin and 250 μin dies represent the rougher ones used in the study. The 60 μin die is included in each plot since the previous plots indicated that the data for this surface roughness appears to represent a transition point. First the dry condition results are presented followed by the lubricated outcomes.

4.2.2.1. Un-Lubricated Results

Figure 4.8 and Figure 4.9 below plots part orientation compared against the length strain for the smoother and rougher dies, respectively. The smoothest die (4 μin) shows a positive proportional relationship while the other two roughnesses on Figure 4.8 are essentially flat. Figure 4.9 shows that the rougher dies actually had less material flow in the secondary direction, by about 0.02 in./in. If just length strain is considered Figure 4.8 and Figure 4.9 show that there is no clear dependence on part orientation except for 4 μin .

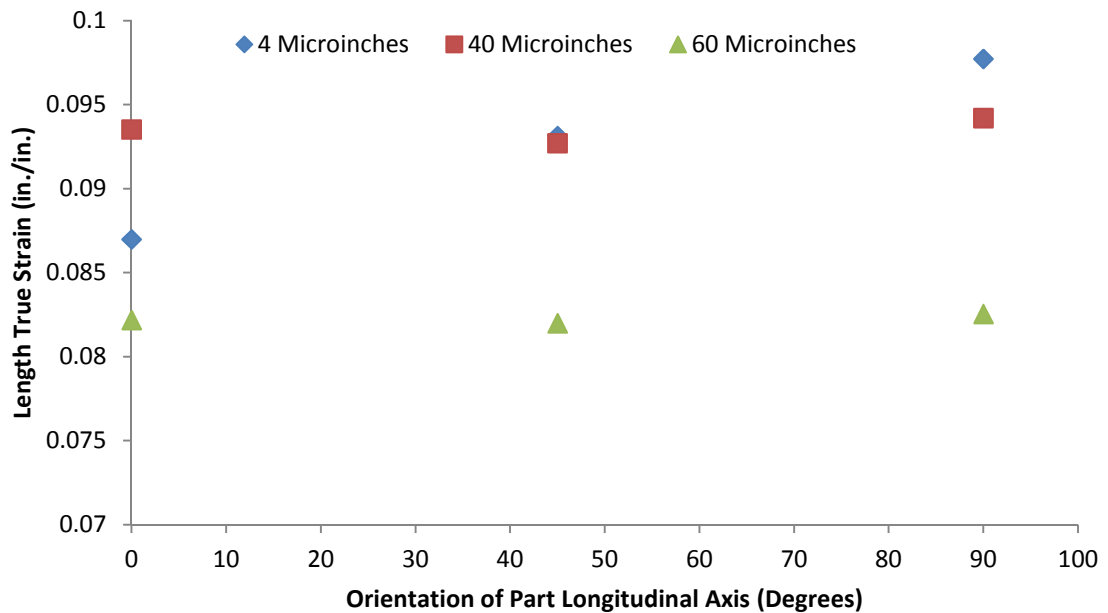


Figure 4.8 - Average length strain as a function of part orientation for smoother dies. Tests were performed without lubrication.

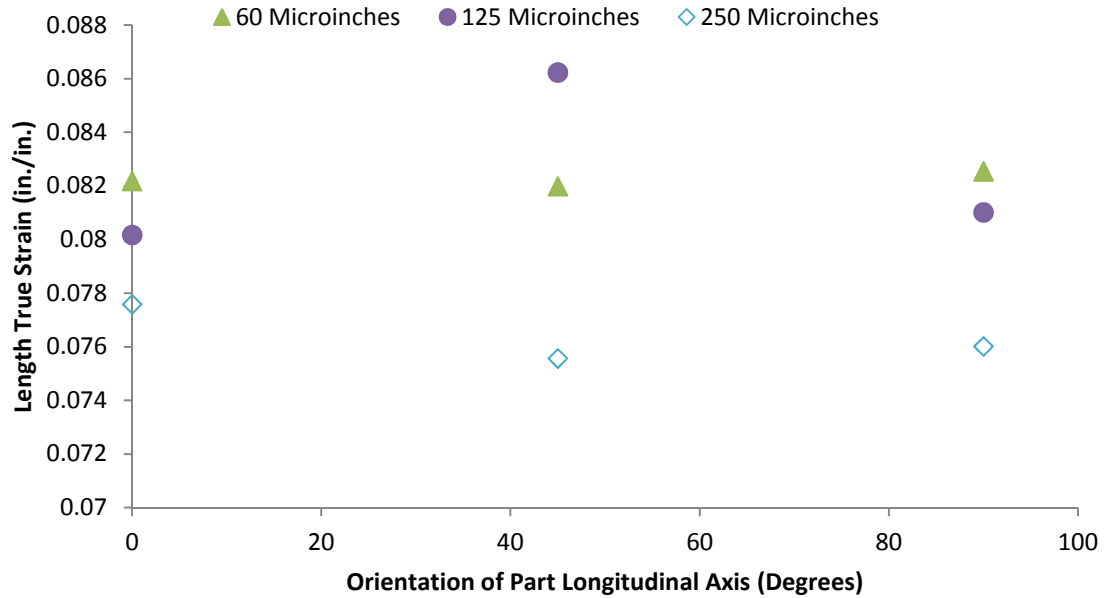


Figure 4.9 - Average length strain as a function of part orientation for rougher dies. Tests were performed without lubrication.

Figure 4.10 and Figure 4.11 below plot the width strain as a function of part orientation for the smoother and rougher dies, respectively. The smoother die width strain is slightly affected by part orientation. A slightly parabolic relationship is evident, with a maximum at the 4 μin and 40 μin die at 45° . The 60 μin plot has the opposite parabolic curve with a minimum at 45° instead. Like in Figure 4.8 and Figure 4.9, the smoother dies result in more width flow than their rougher counterparts again by about 0.05 in./in. The result compares well to the dependence of part lay to die roughness found by Menezes et al. [23] for the smoother surfaces.

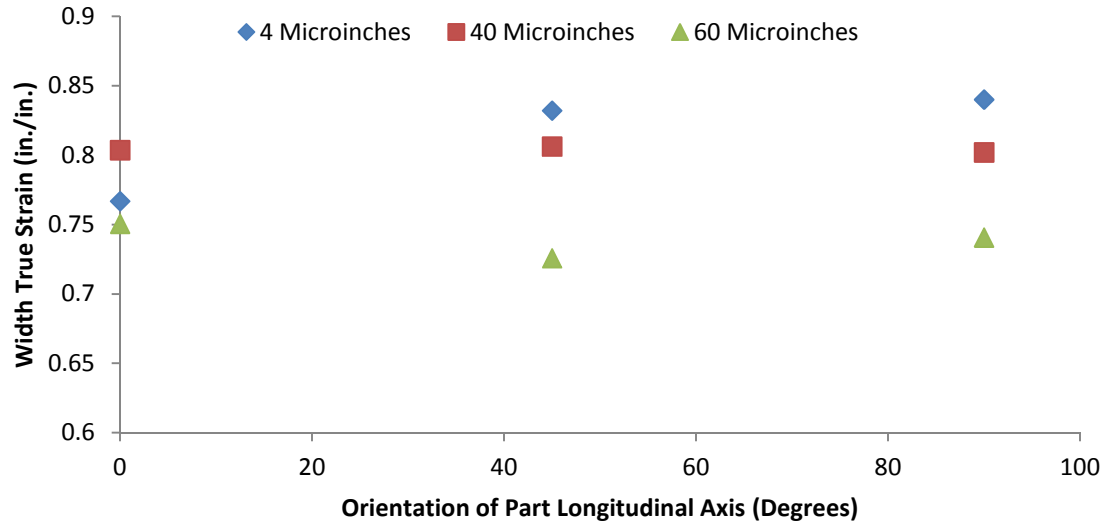


Figure 4.10 - Average width strain as a function of part orientation for smoother dies. Tests were performed without lubrication.

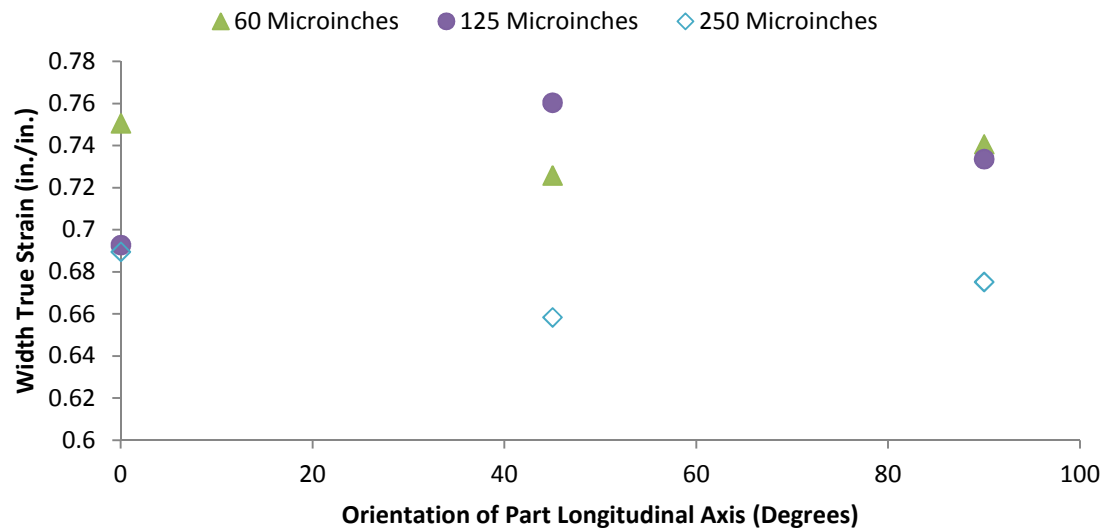


Figure 4.11 - Average width strain as a function of part orientation for rougher dies. Tests were performed without lubrication.

Figure 4.12 and Figure 4.13 below are the spread ratios as a function of part orientation for the smoother and rougher dies, respectively. Considering the 4 μm die, having the long axis perpendicular to the grinding direction appears to result in the

greatest flow. But this trend does not seem to continue to each roughness and seems to change at 60 μin .

While further investigation is warranted, some correlation between flow and orientation is evident from the experimental data. It is interesting to note that at lower values of roughness a maximum point occurs at the 45-degree orientation but this shifts towards the 90-degree value at the highest roughness values tested. It is unclear as to the reason but the 60 μin value seems to represent a transition point from a non linear to linear relationship. This trend tends to mirror results reported by Rabinowicz [17] where a plot of coefficient of friction against roughness shows a negative slope region caused by excessive junction growth for smooth finishes, and a positive region caused by interlocking of asperities at high values of surface roughness with friction being independent of roughness in the intermediate region. However those results reported by Rabinowicz were completed using a copper pin and a copper disk, so direct application to this study is difficult. As reported in Chapter 3, the work pieces used in this study had an average surface roughness of 35 μin , so the asperity contact for the 60 μin through 4 μin dies appears to be reasonable. The rougher work piece would have deeper or more asperities that need to be traversed before more deformation can occur. Additionally, these results are confirmed by the investigation completed by Menezes et al. [23] which indicated a strong dependence of friction factor on grinding angle.

For the two higher die surface roughness values (125 μin and 250 μin) a different mechanism develops. As discussed in Chapter 3, platens were machined with grooves to create a high roughness that approximated a greatly roughened, worn die surface. It would appear that as the orientation angle increases, the spread ratio also increases, albeit

very slightly. The grooves represent an added barrier to flow in both directions, causing the material to first bridge the gap before continuing to flow outwards. The trend supports this concept, since the number of perpendicular boundaries to the width strain increases as the angle increases.

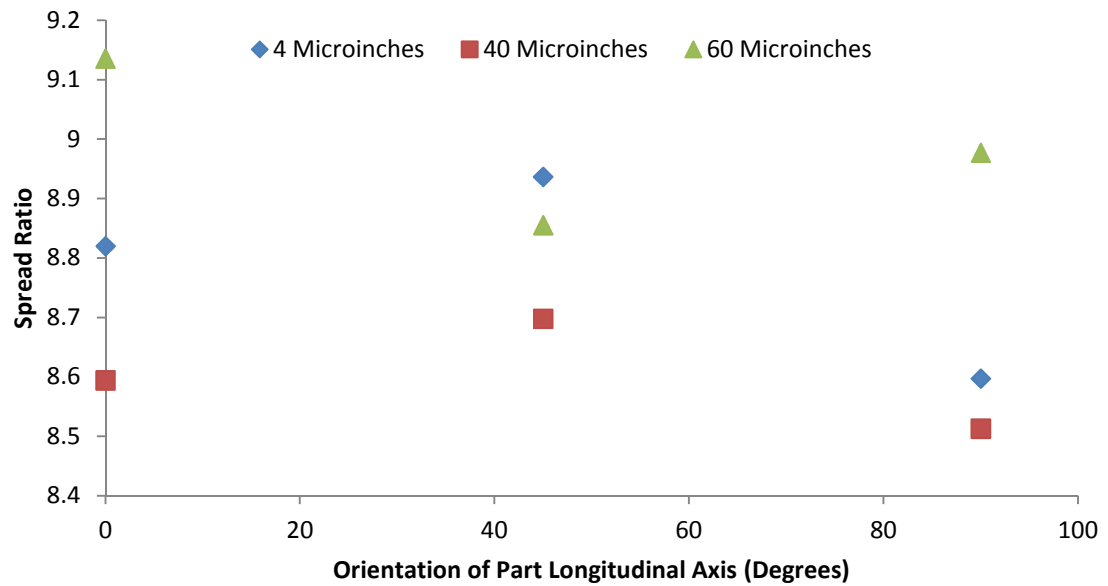


Figure 4.12 - Average spread ratio as a function of part orientation for smoother dies. Tests were performed without lubrication.

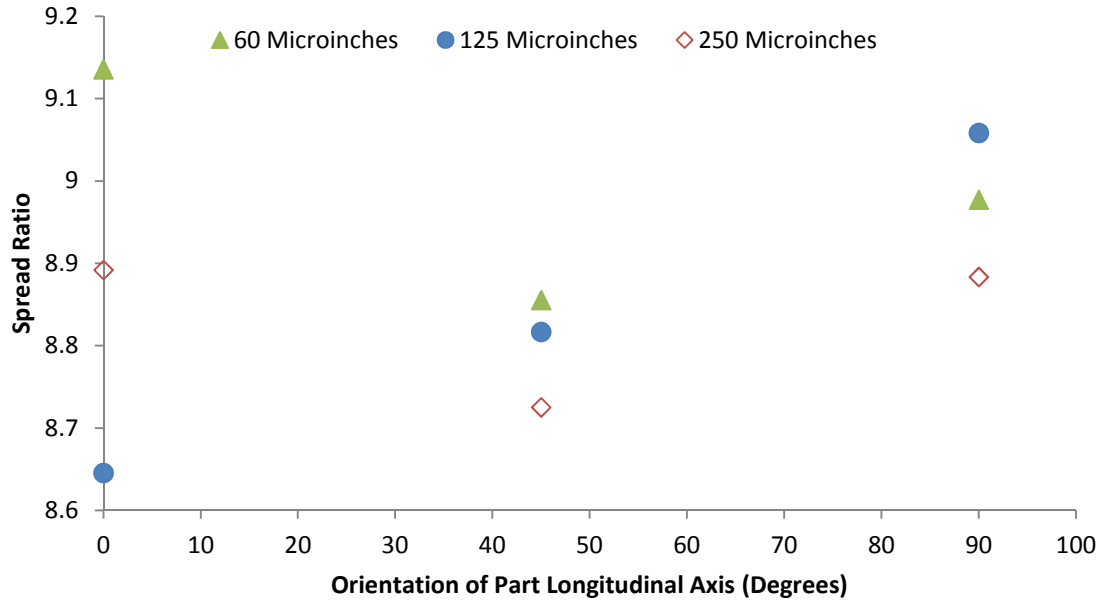


Figure 4.13 - Average spread ratio as a function of part orientation for rougher dies. Tests were completed preformed lubrication.

To further illustrate the concept of “gap bridging”, refer to Figures 4.16 through 4.26 below. The arrows represent the flow in the width dimension and notice how as the orientation changes from 0 degrees to 90 degrees, the number of gaps the material has to cross increases. If the total upset height is fixed, then if the material has to flow more to bridge the gaps, then the overall material flow and therefore spread would be less. To further explore this phenomena, a model was created in DEFORM to simulate the current test conditions and observe the material flow over these gaps. The next section addresses the details of the analysis.

Overall, it would appear that there is not much difference in this suspected phenomenon from a R_a of 125 μin to 250 μin . Both of the spread ratios in Figure 4.13 trend upwards but there is not a significant offset between the two roughnesses to believe

one leads to more or less material flow. It seems that the action of going over the gap has more influence on flow than the total number of gaps.

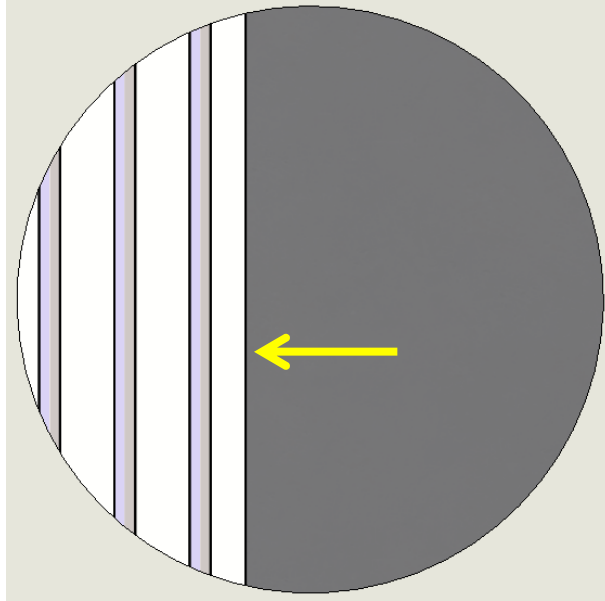


Figure 4.14 – A close-up die view showing a cigar specimen and the arrow showing the width flow direction at 0 Degrees (Long axis parallel to grooves). Note that the darkened region represents a very close detailed side top view of the cigar specimen.

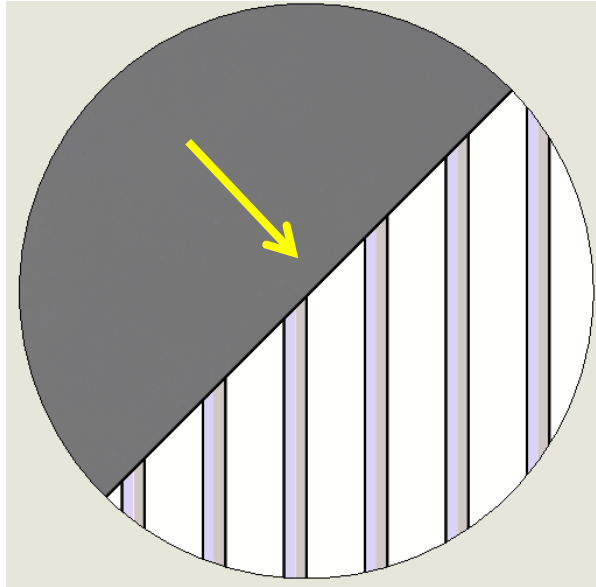


Figure 4.15 - A close-up die view showing a cigar specimen and the arrow showing the width flow direction at 45 Degrees. Note that the darkened region represents a very close detailed side top view of the cigar specimen.

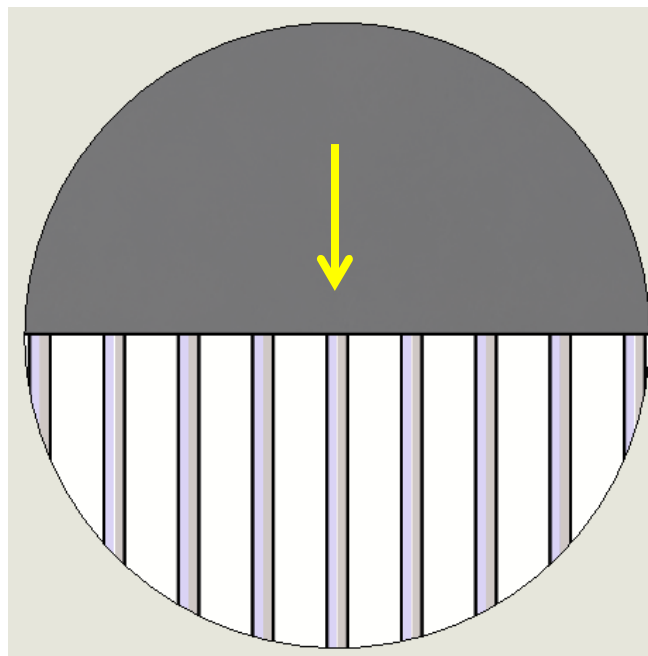


Figure 4.16 - A close-up die view showing a cigar specimen and the arrow showing the width flow direction at 90 degrees (Long Axis Perpendicular to Grooves). Note that the darkened region represents a very close detailed side top view of the cigar specimen.

4.2.2.2. Testing With Lubricant

Presented below are the average length and width strains and spread ratio results of the cigar testing completed with lubricant. All the same test procedures were used, but with the addition of lubrication using the methodology described in section 3.4.2. For clarity, each plot of broken into a rougher die and smoother die plot and the error bars removed. All standard deviation data can be found in Appendix C.

Figure 4.17 and Figure 4.18 below again are the length strains plotted as a function of part orientation, but with the addition of lubricant. When compared to the results obtained in the dry condition (Figure 4.8 and Figure 4.9), a definitive upward shift is observed which means the material had increased flow in the length direction. The length strain increased on average around 0.011, while the overall negative relationship between die roughness and length true strain still exists. The same overall slope with an increase in strain also lends credence to the overall repeatability of the experiment as well as the mechanisms at work.

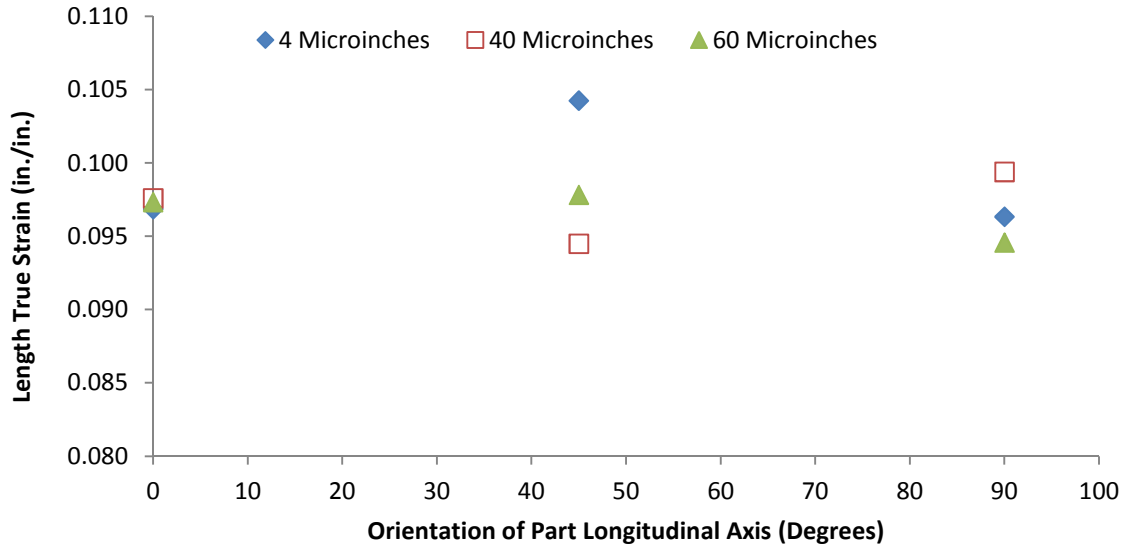


Figure 4.17 - Average length strain as a function of part orientation for smoother dies. Tests were performed with lubrication for the rectangular specimens.

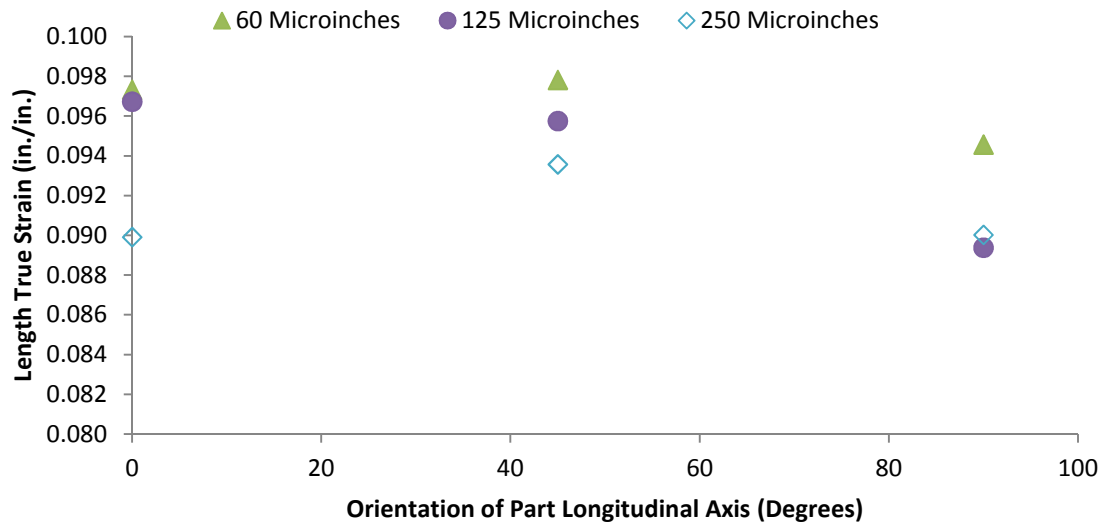


Figure 4.18 – Average length true strain as a function of part orientation for rougher dies. Tests were performed with lubrication for the rectangular specimens.

Figure 4.19 and Figure 4.20 below show the smoother and then rougher die width strain as a function of part orientation when lubricant was used in the testing. Just like the length strains, an increase in width strain on the order of 0.018 is observed with the use of

lubricant. More importantly, the same trends that are seen without of the use of lubricant in Figure 4.10 and Figure 4.11 are observed when a lubricant was used. Figure 4.19 shows that there is a nonlinear relationship between part orientation and roughness with the 4 μin die having a downwards parabolic relationship and the 40 μin having a positive. Again, the 60 μin is shown as a transition point, being both slightly parabolic and linear.

The rougher dies, as shown in Figure 4.20, have a positive linear relationship, which matches the one observed in Figure 4.11. The use of lubricant helped to increase overall material flow without effecting the previously mentioned gap bridging flow mechanism.

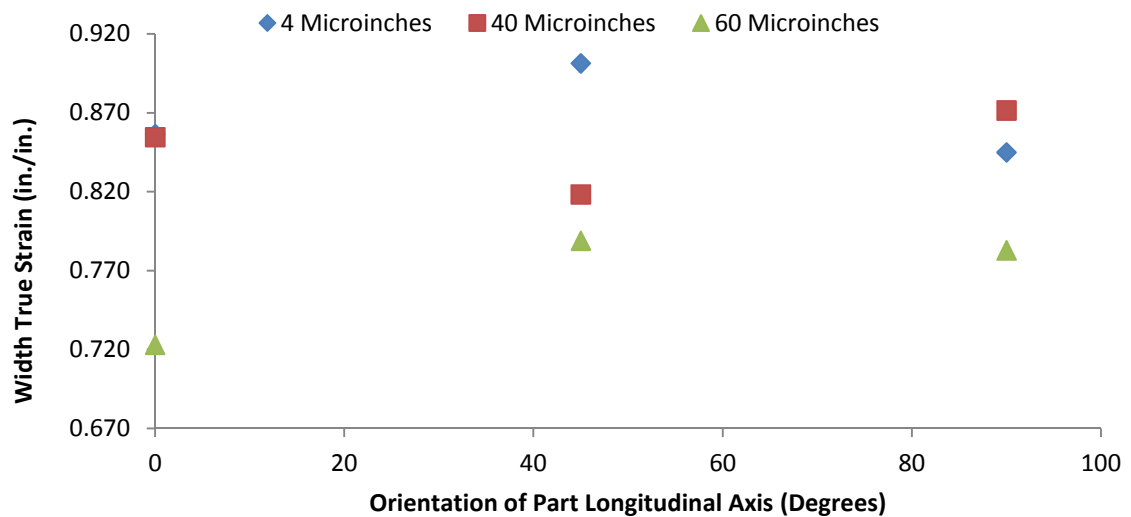


Figure 4.19 - Average width strain as a function of part orientation for smoother dies. Tests were performed with lubrication.

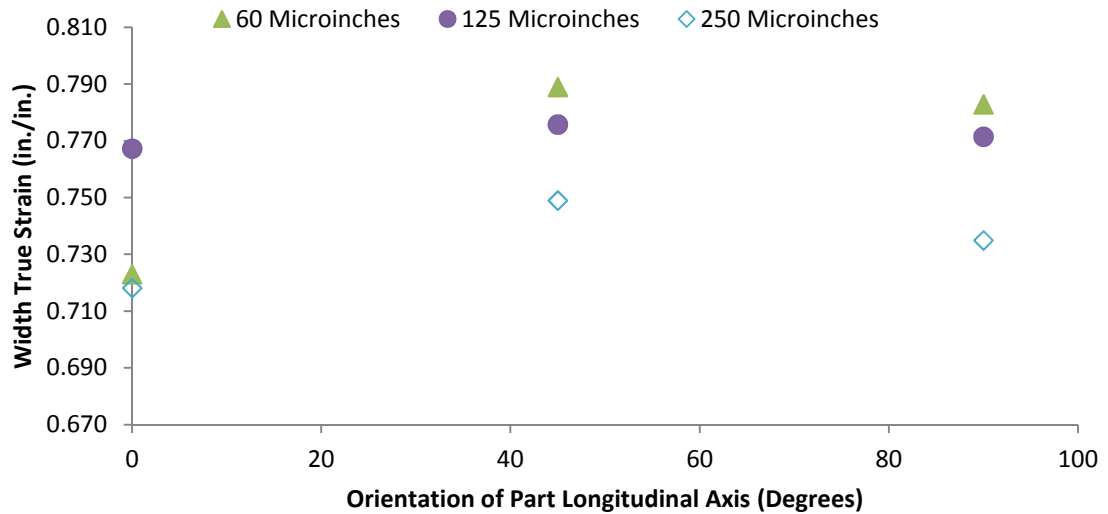


Figure 4.20 - Average width true strain as a function of part orientation for rougher dies. Tests were performed with lubrication.

Figure 4.21 and Figure 4.22 below shows the spread ratio plotted as a function of part orientation for the smoother and then rougher dies, respectively, with the use of lubricant. Like the spread ratios in Figure 4.12 and Figure 4.13 under dry conditions, two distinct relationships exist. The lower surface roughness values, 4 μin and 40 μin , had a slightly parabolic trend but generally the trend is linear as Figure 4.20 shows for the other three roughnesses. Similar to the examination of average spread ratio as a function of surface roughnesses, the average spread ratio actually decreased by about 0.50 for each roughness when using lubricant. Again, this decrease is explained by the length strain increasing more than the width strain. The lubricant helped to reduce friction but appears to have aided more in the secondary than the primary direction. One of the concerns with using lubricant was ensuring that it was applied to a reasonable consistency on the surface of both platens. After inspection of the dies and specimens and the observation of repeated non-linear and linear trends for the smoother and rougher dies, respectively, it

was concluded there was not a significant buildup of lubricant throughout testing. If there were heavily lubricated spots on the die, the parts would have deformed more in certain areas and shifting the data significantly.

However, the higher levels of roughness, 125 μin and 250 μin , again had a positive relationship when it came to the effect of orientation as shown in Figure. This fact means that the lubricant did not fill the machined gaps enough to create a “bridge” of sorts and reducing the gap jumping and curl observed in the dry state. 60 μin again represent a type of transition from the micro-effects of asperity contacts to the macro-effects of the gaps caused by machining. The trend is positive with respect to part orientation, but there is still some parabolic shape to the data.

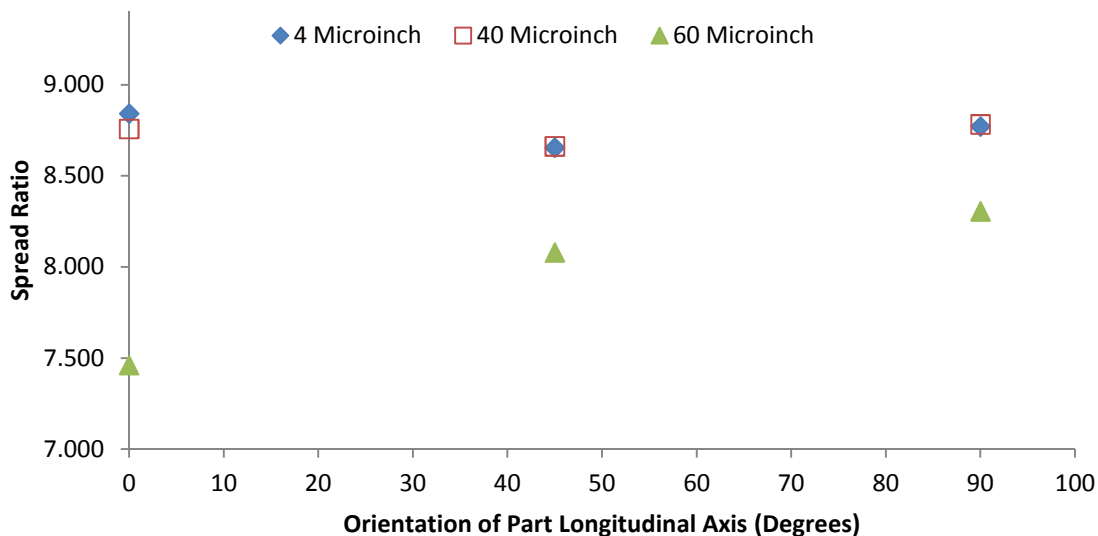


Figure 4.21 - Average spread ratio as a function of part orientation for smoother dies. Tests were performed with lubrication.

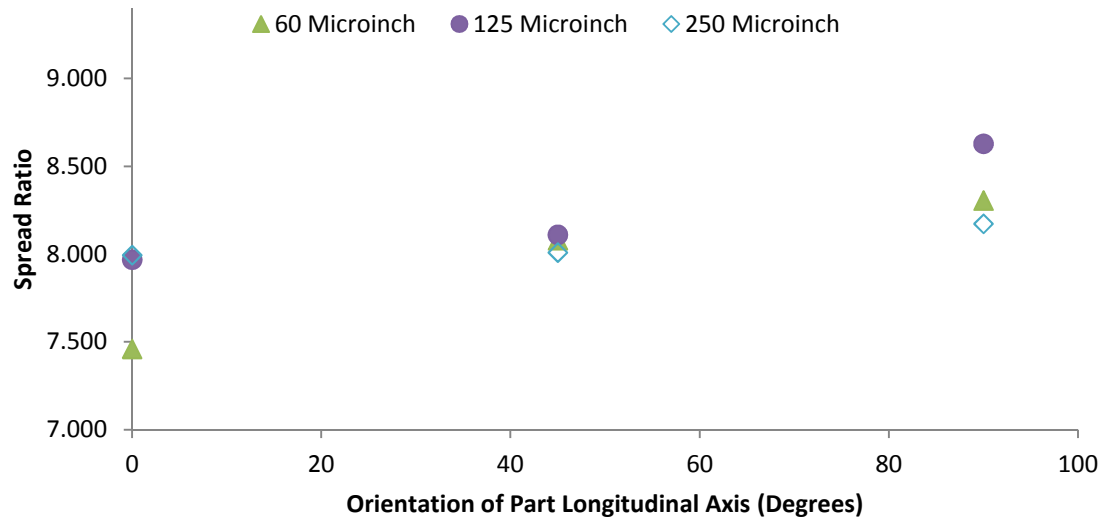


Figure 4.22 - Average spread ratio as a function of part orientation for rougher dies. Tests were performed with lubrication.

4.2.3. DEFORM Finite Element Analysis

To gain more detailed insight as to how metal movement was affected by surface roughness, DEFORM (Scientific Forming Technologies Corporation, Columbus, OH), a commercial Finite Element Analysis code, was used to study the local metal flow in the vicinity of the die surface during the compression of a cigar test specimen. The analysis was run under both isothermal and non-isothermal conditions.

The simulation was completed in two-dimensions because it was not possible to obtain satisfactory resolution using a three-dimensional model without using an excessive number of elements. The two-dimensional model assumed plane strain conditions which reasonably approximate conditions in the cigar test. The length strain was assumed to be zero to hold the plane strain assumption, which is reasonable since the length strains observed in the tests were generally less than 10% of the length. Since the cigar

specimen has two-fold symmetry, planes of symmetry were used in order to optimize resolution and the number of elements needed in the model. Planes were positioned along coordinated coinciding with the horizontal and vertical midpoints, essentially breaking the part into four symmetric rectangular measuring 0.125" by 0.125". Figure 4.23 below is a picture of the initial setup before any deformation was calculated. The aluminum specimen was meshed using 5100 quadrilateral elements and the 125 μin R_a surface was simulated. The mesh was distributed to further optimize resolution by placing more elements at the die surface than in the interior of the specimen. Figure 4.24 below is a picture of the final simulation time step, showing the overall change in the simulated work piece geometry and it can be seen that some bulging is evident.

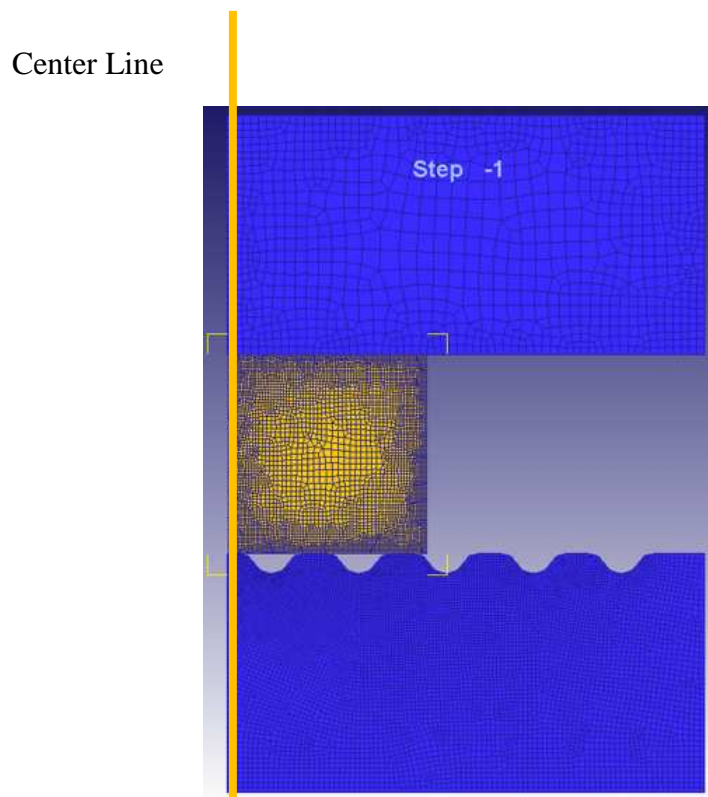


Figure 4.23 – Two-dimensional, plane strain, non-isothermal FE model of the cigar test with surface roughness of 125 μin platens. The line to the left of the model represents the centerline of the part and a plane of symmetry.

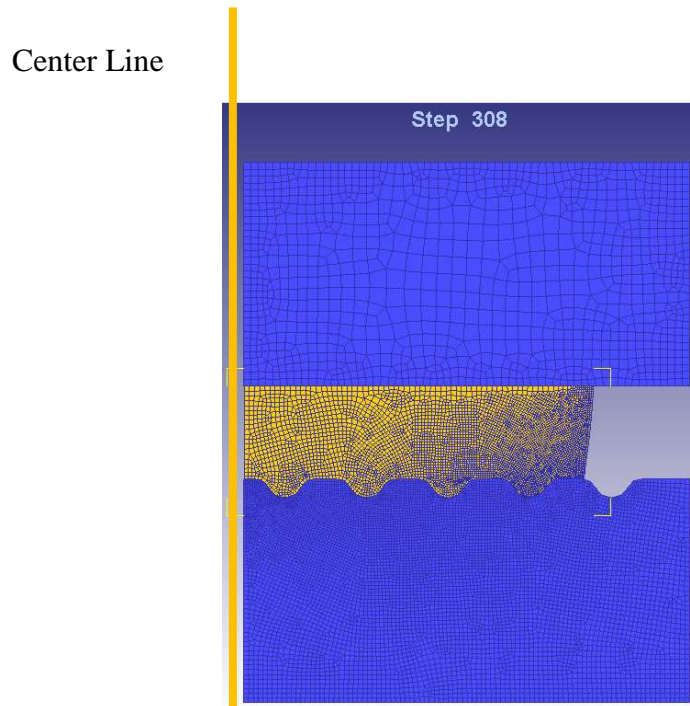


Figure 4.24 - The DEFORM model of the cigar test after deformation was complete.

In order to limit simulation time and the number of elements, the $125\ \mu\text{m}\ R_a$ die was chosen for the simulation since it was smoothest roughness that was practical to model using the DEFORM software. The die surface used in the model was an approximation, based on the schematic in Figure 3.6. Enhancements, like corner radii to minimize the possibilities of numerical singularities, were needed to increase resolution and the die surface roughness was approximated using a sine wave. The work piece was meshed such that a minimum of three elements were used to bridge each groove so that satisfactory local flow behavior resulted from the model. Additionally, friction factor on the die surface was modeled as a constant 0.7 to reflect the dry conditions used during experimental testing. A frictionless condition was specified for the top die to reflect the symmetry plane. All other inputs for the software, such as die travel, forging speed, die and work piece temperatures were identical to conditions used in the experimental

procedure. In this specific simulation, a cross section of 0.25 in. x0.25 in of a cigar specimen in the parallel (0 degree) orientation was chosen which corresponds to the work piece width. The parallel orientation was used since it was the only angle that could practically be simulated in using a plane strain representation. Figure 4.25 below shows the deformed mesh and velocity vectors at selected time steps from the non-isothermal simulation.

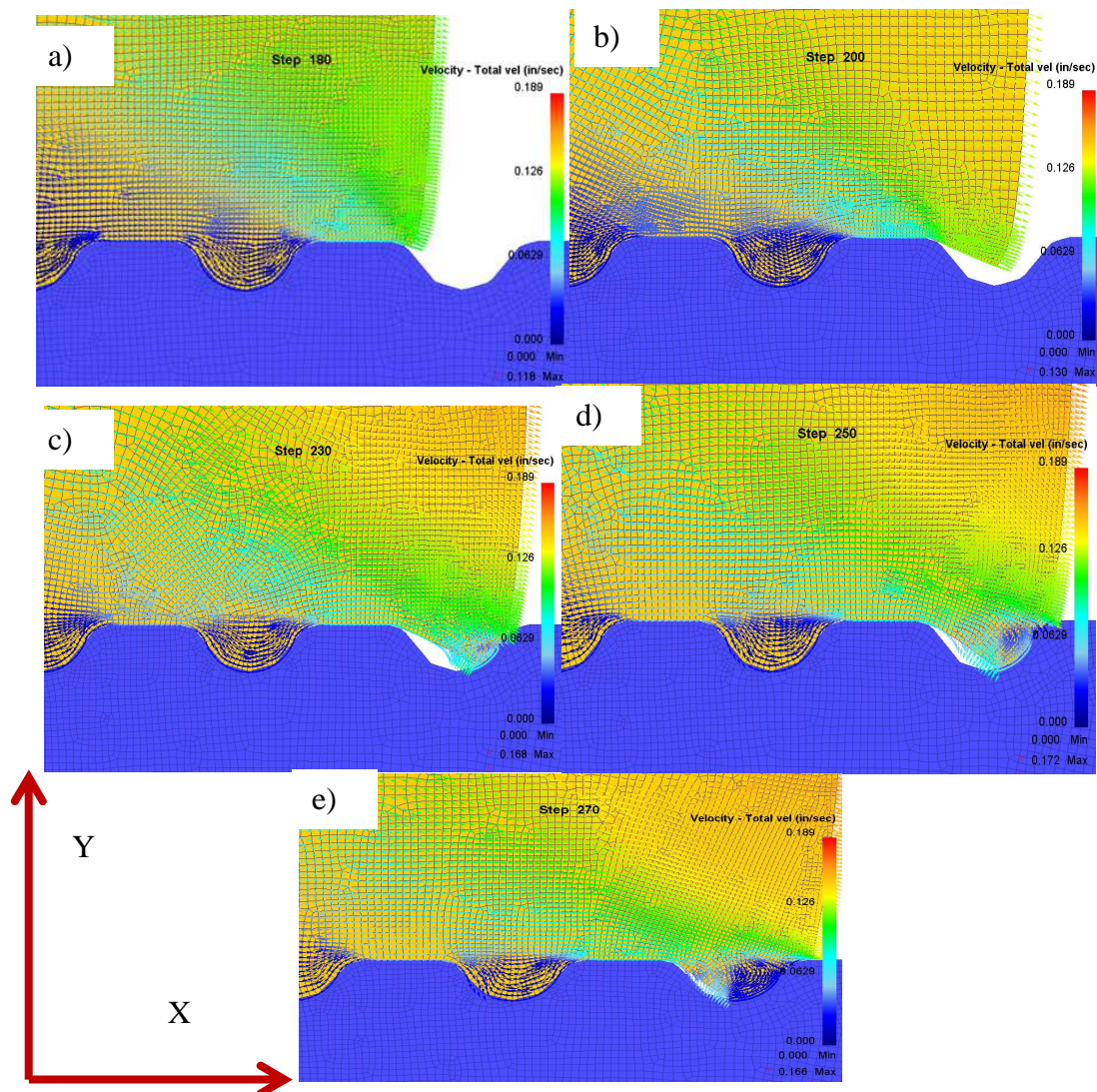


Figure 4.25 – Velocity field results from DEFORM 2D of cigar specimen orientated at 0 degrees. The same coordinate axis is shown in the lower right of the group of pictures. The model progresses alphabetically (a through e) and show the progress of the specimen bridging the groove in the X direction and then curling upwards in the Y direction.

Examining the simulation sequence, it can be seen that from Step 0 to about Step 180, corresponding to 0 to 71% of the total die travel, the material primarily flows downward in the negative y-direction, filling in the grooves on the die surface with minimal lateral material flow in the horizontal direction. Once the grooves located directly below the part surface are filled, dead metal zones start to appear, which is observed in the upper right picture in Figure 4.25 a) as the darkened area where the velocity has decreased to near 0. The dead metal causes the part to shear laterally and downward in the negative-y direction, which is seen as the light-blue area in the picture of Figure 4.25 a).

When the material encounters the gap from 71% to 82% of total die travel (picture a) to b) of Figure 4.25), instead of filling downwards in the y-direction, it flows laterally in the positive x-direction and down slightly in the y. Then the material flows into the other side of the groove, filling downward in the y-direction and back towards the leading edge of the groove in the negative x-direction from 88% to 90% of total die travel (picture c) to d) of Figure 4.25). Finally, the material curls back onto itself at 92% of total die travel (picture e) of Figure 4.25). The curl back up in the positive y-direction slows down the material at the subsurface, which then retards flow in the width direction. The slowdown in subsurface flow causes shearing of the material at this interface. The material shear further reduces material movement, since significant energy from the press is now causing more internal shearing rather than lateral flow.

To confirm the results from the DEFORM simulation, an aluminum sample was sectioned, mounted, and examined under a 10X magnification optical microscope. Figure 4.26 below has an arrow pointing to an area of suspected curling in the gap filling

area. If the material was flowing towards the right of the picture, the slightly downward slope and then sharp turn upwards is explained by the gap bridging observed in DEFORM.

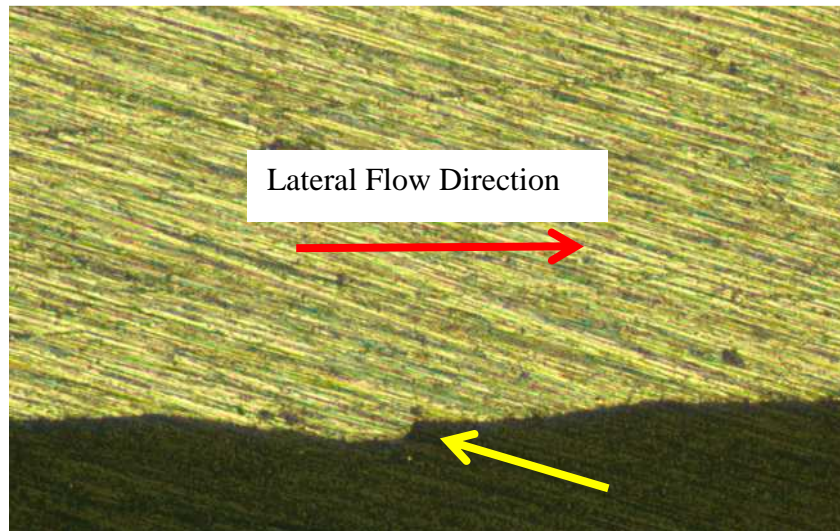


Figure 4.26 – 10X magnification of a cross section of a cigar test specimen. There appears to be some curl in the noted area.

4.3. Ring Testing Results and Discussion

The following is a presentation of the results obtained from the ring compression testing that was conducted. The friction factor was obtained using the correlation that Male and Cockcroft found for coefficient of friction which was then converted to friction factor assuming the material obeyed the von Mises yield criteria.

4.3.1. Dry Results

Figure 4.27 below plots the results of the ring test using a 60 μin die and die temperatures ranging from 250 $^{\circ}\text{F}$ to 400 $^{\circ}\text{F}$ in 50 degree increments. It can be seen from

Figure 4.27 that the friction factor increased in direct proportion to the die temperature that was used in the ring compression test. This result helps to confirm the results of the cylindrical upset testing which showed an increase in the radius of curvature with the die temperature. The linear trend is confirmed by a regression curve that was fitted to the data which shows a very strong measure of fit based on R^2 value of 0.97699. While increasing the die temperature helps to lessen the amount of die chilling that occurs on the part, as explained in section 4.1 of this chapter, the increased die temperature promotes oxide layer thickness growth as well as an increase in the affinity for the tool steel and aluminum to adhere to each other. Again, the die platens were inspected after testing for signs of plowing and micro welding but no buildup or residue from the aluminum work piece was found. The likely increase of the two materials' affinity for adherence means that any decrease in flow stress from decreased die chilling was overshadowed.

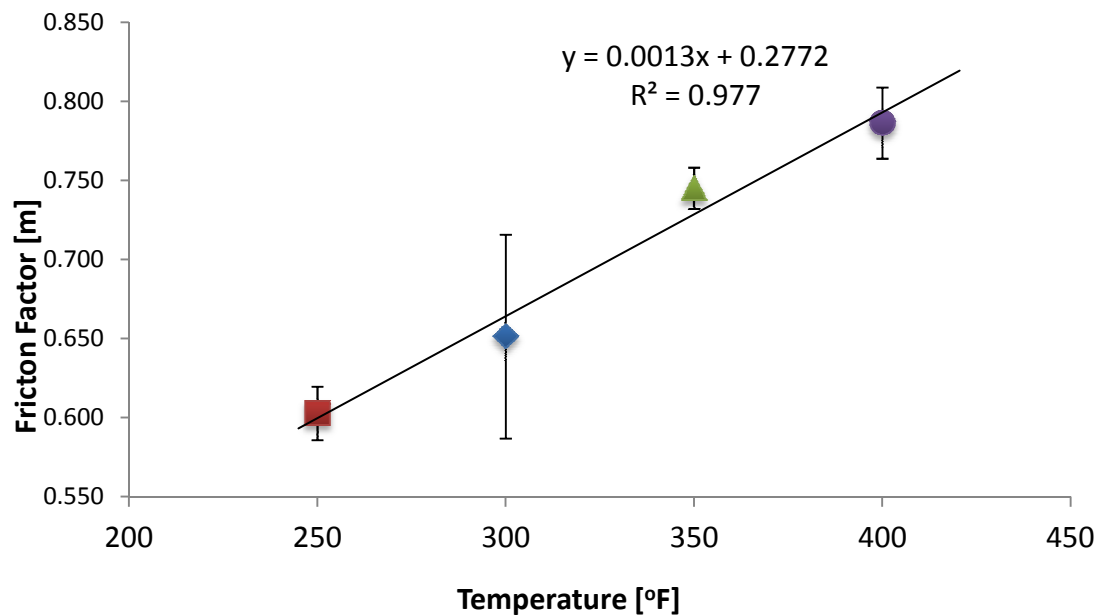


Figure 4.27 - Ring compression test results shown as friction factor as a function of die temperature completed on a $60 \mu\text{in } R_a$ concentric die.

Figure 4.28 below shows the results of the ring compression test for the various dies that were used for the cigar test portion of the study. When examining just the dies that were machined using a surface grinder, the friction factor appears slightly parabolic. A maximum value of friction factor is observed at 40 μin while lower values occur at 4 μin and 60 μin . This parabolic nature helps to confirm the transition point that occurs in the spread ratio figures in section 4.2. When considering the 60 μin , 125 μin and 250 μin dies, the relationship is more linear in nature and there does not appear to be a major effect caused by the roughness with respect to friction factor. All the friction factors for these dies seem to be in the 0.775 range, with a slight increase at the 125 μin die. Overall, the friction factor appears to be independent of surface roughness for R_a values in excess of 60 μin . Additionally, Figure 4.28 appears to suggest a minimum friction factor value of 0.779 at 60 μin which empirically supports the value typically being used in industry for machining forging dies.

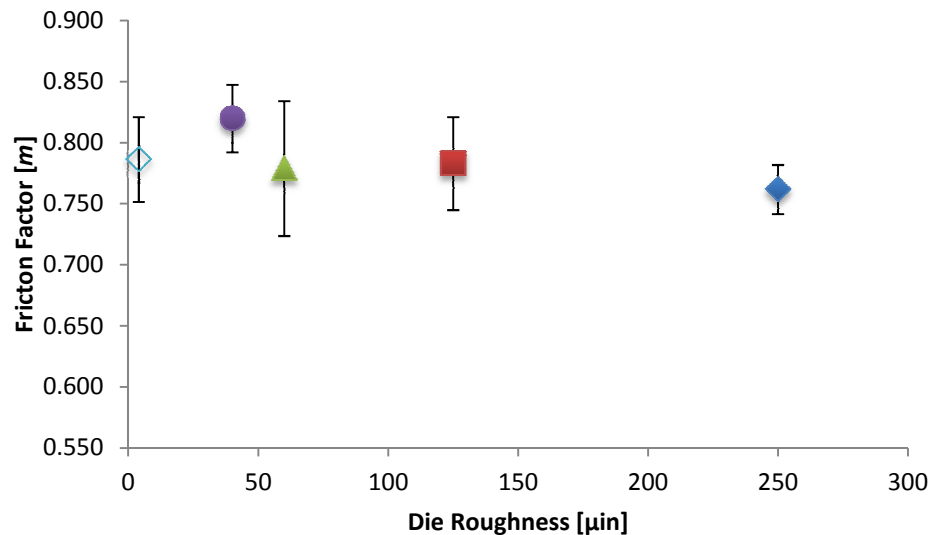


Figure 4.28 - Ring compression test results shown as friction factor as a function of die surface roughness at 400°F die temperature. Performed in the dry condition (No Lubricant).

4.3.2. Lubricant Results

Figure 4.29 below shows the ring test results that were completed using a water-graphite lubricant. Again, the lubricant was applied via the method described in section 3.4.2. The same parabolic-type trend for the 4 μin , 40 μin , and 60 μin dies is observed, although the curve is shifted downward. The shift suggests that the lubricant did help to reduce the asperity contact causing a portion of the observed friction factor. Additionally, any exposed un-oxidized aluminum as a result of the deformation would be buffed from the die by the lubricant also helping to reduce any effects between the fresh aluminum and die sticking. However, it did not help to completely eliminate these phenomena because the same parabolic trend observed under dry testing conditions is still evident. Looking at the three rougher dies, 60 μin , 125 μin and 250 μin , the same linear trend is seen. But, just like the parabolic trend, a downward shift occurs, placing all three means near a friction factor value of 0.7. The shift reaffirms the general mechanisms at work and that the lubricant did help to lower the overall observed friction in the part/die system. Again, friction factor appears to be independent of R_a at the rougher die surfaces.

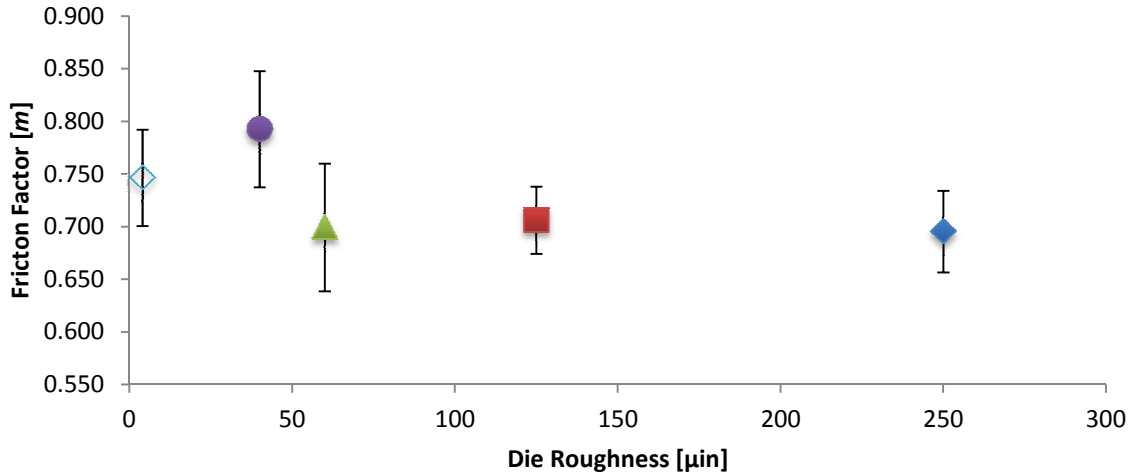


Figure 4.29 - Ring compression test results show as friction factor as a function of die surface roughness at 400°F die temperature. All the tests were conducted using lubricant.

5. Summary and Conclusions

Overall, this study explored the relationship between material flow and surface roughness in hot forging applications. By using the ring compression test and cigar test, an experimental investigation was conducted to explore if part orientation with respect to a die's roughness can be used to influence metal flow. A DEFORM model was also used to gain a better perspective of the local metal flow behavior at the die/part interface during the cigar test. The ring compression test was used again with the cylindrical upsetting test to find a relationship between die temperature and friction factor. All of these tests were conducted using 6061-T6 aluminum on an instrumented die set using a 10-ton hydraulic press.

Based on the results obtained, it can be concluded that:

- Friction factor for the aluminum specimens are directly proportional to die temperature. An increase in die temperature resulted in an increase in the friction factor for un-lubricated die surfaces.
- Die roughness above 60 μin result in a directly proportional relationship of material flow to part orientation with respect to die surface lay. For die roughness below 60 μin , a nonlinear relationship is evident with a transition in material flow at 45°.
- The linear relationship of lay to material flow at roughnesses above 60 μin is caused by lateral flow across a die groove and then curling back towards a dead metal zone resulting in increased resistance to flow.
- Use of lubricant helps to lower overall friction factor but does not influence material flow compared to surface roughness or part orientation in a way that eliminates the trends observed in dry conditions.
- Part lay does have a potential use in forging die design, but it is a second order effect. Die roughness still dominates overall effects on material flow and therefore is likely more useful in forging die design.

6. Recommendations for future work

Going forward, there are still several areas where additional investigation is needed regarding the effect of die roughness and temperature on material flow. First, it is recommended that the cigar tests be repeated over a range of die temperatures to determine if the results observed here are valid. If temperature is introduced into the completed cigar testing, the effect of all three parameters can be examined and a more accurate relationship between these factors determined. Another area of this study that is open for more investigation is the relationship between die temperature and friction factor. The direct cause of the increase of friction as die temperature increased could not be determined since no visible buildup of aluminum or abnormal wear on the tool steel was observed. If the study was repeated using other materials, it could also be determined if the positive relationship between the two is observed only due to the aluminum oxide or if other oxides change the trend. More study is also needed on how aluminum oxide affects friction at the die/work piece interface during forming. The sudden increase in friction factor in both dry and lubricated conditions for the 40 μm die is another area where additional investigation is needed.

Furthermore, finding geometry more complex than a rectangle could introduce another parameter for material flow. However, this does complicate the analysis portion since additional constraints to flow, like corners, would have to be considered and controlled. The positive side to all the analysis would help bring the study closer to actual forging applications observed in industry. Moreover, a more controlled lubrication application should be developed and used in lab-based studies which can bring a study closer to actual application. Since lubricant is used as the status quo in industry, finding

the effects of roughness when a die has a variable amount of it would be highly beneficial and help die designers optimize their lubricant systems.

7. References

- [1] Groover, M.P., 2010, "Fundamentals of Modern Manufacturing: Materials, Processes, and Systems," John Wiley & Sons, Hoboken, NJ, pp. 88, Chap. 5.3.2.
- [2] Schey, J.A., 1983, "Tribology in Metalworking: Friction, Lubrication, and Wear," American Society for Metals, Metals Park, Ohio, pp. 443.
- [3] Faunce, J. P., Lockwood, F. E., and Boswell, W., 1983, "Selecting and Evaluating Lubrications for Forging Alumium," *Lubrication Engineering*, **39**(12), pp. 761-765.
- [4] Barykin, N. P., and Semnov, V. I., 1994, "Metal-Cladding Commerical Lubricants for Hot Forging of Alumium-Based Alloys," *Material Science Forum*, **170-172**, pp. 787-792.
- [5] Sahin, M., Çetinarslan, C. S., and Akata, H. E., 2007, "Effect of Surface Roughness on Friction Coefficients during Upsetting Processes for Different Materials," *Materials & Design*, **28**(2), pp. 633-640.
- [6] Dutton, R. E., Seetharaman, V., Goetz, R. L., 1999, "Effect of Flow Softening on Ring Test Calibration Curves," *Materials Science and Engineering: A*, **270**(2), pp. 249-253.
- [7] Douglas, J. R., and Altan, T., 1975, "Flow Stress Determination for Metals at Forging Rates and Temperatures," *Journal of Engineering for Industry, Transactions of the ASME*, (Feburary), pp. 66-76.
- [8] Altan, T., and Lee, C. H., 1972, "Influence of Flow Stress and Friction upon Metal Flow in Upset Forging of Rings and Cylinders," *Journal of Engineering for Industry, Transactions of the ASME*, **94**(3), pp. 775-782.
- [9] Male, A. T., and Cockcroft, M. G., 1964, "A Method for the Determination of the Coefficient of Friction of Metals Under Conditions of Bulk Plastic Deformation," *Journal of the Institute of Metals*, **93**, pp. 38.
- [10] Schroeder, W., and Webster, D. A., 1949, "Press-Forging Thin Sections: Effect of Friction, Area, and Thickness on Pressures Required," *Journal of Applied Mechanics*, (16), pp. 289.
- [11] Fricker, D. C., and Wanheim, T., 1974, "Low Friction Coefficient Estimation for Model Material Experiments," *Wear*, **27**, pp. 303-317.
- [12] Schey, J. A., Venner, T. R., and Takomana, S. L., 1982, "The Effect of Friction on Pressure in Upsetting at Low Diameter-to-Height Ratios," *Journal of Mechanical Working Technology*, **6**(1), pp. 22-33.

- [13] Malayappan, S., and Narayanasamy, R., 2004, "An Experimental Analysis of Upset Forging of Aluminium Cylindrical Billets Considering the Dissimilar Frictional Conditions at Flat Die Surfaces," *International Journal of Advanced Manufacturing Technology*, **23**(9), pp. 636-643.
- [14] Malayappan, S., and Narayanasamy, R., 2003, "Observations of Barrelling in Aluminium Solid Cylinders during Cold Upsetting using Different Lubricants," *Materials Science & Technology*, **19**(12), pp. 1705-1708.
- [15] Baskaran, K., Narayanasamy, R., and Arunachalam, S., 2007, "Effect of Friction Factor on Barrelling in Elliptical Shaped Billets during Cold Upset Forging," *Journal of Materials Science*, **42**(18), pp. 7630-7637.
- [16] Li, Y., Onodera, E., and Chiba, A., 2010, "Friction Coefficient in Hot Compression of Cylindrical Sample," *Materials Transactions*, **51**(7), pp. 1210-1215.
- [17] Rabinowicz, E., 1995, "Friction and Wear of Materials," Wiley, New York, .
- [18] Simon, L., McMahon, H. O., and Bowen, R. J., 1951, "Dry Metallic Friction as a Function of Temperature between 4.2K and 600K," *Journal of Applied Physics*, **22**(2), pp. 177-184.
- [19] Leu, D., 2011, "Modeling of Surface Roughness Effect on Dry Contact Friction in Metal Forming," *International Journal of Advanced Manufacturing Technology*, **57**(5-8), pp. 575-584.
- [20] Mahrenholtz, O., Bontcheva, N., and Iankov, R., 2005, "Influence of Surface Roughness on Friction during Metal Forming Processes," *Journal of Materials Processing Technology*, **159**(1), pp. 9-16.
- [21] Dubar, L., Hubert, C., and Christiansen, P., 2012, "Analysis of Fluid Lubrication Mechanisms in Metal Forming at Mesoscopic Scale," *CIRP Annals - Manufacturing Technology*, **61**(1), pp. 271-274.
- [22] Becker, P., Jeon, H. J., and Chang, C. C., 2003, "A Geometric Approach to Modelling Friction in Metal Forming," *CIRP Annals - Manufacturing Technology*, **52**(1), pp. 209-212.
- [23] Menezes, P. L., Kishore, and Kailas, S. V., 2010, "Response of Materials as a Function of Grinding Angle on Friction and Transfer Layer Formation," *International Journal of Advanced Manufacturing Technology*, **49**(5-8), pp. 485-495.
- [24] Menezes, P. L., Kishore, and Kailas, S. V., 2009, "Influence of Surface Texture and Roughness Parameters on Friction and Transfer Layer Formation during Sliding of Aluminium Pin on Steel Plate," *Wear*, **267**(9-10), pp. 1534-1549.

- [25] Bay, N., Eriksen, M., Tan, X., 2011, "A Friction Model for Cold Forging of Aluminum, Steel and Stainless Steel Provided with Conversion Coating and Solid Film Lubricant," *CIRP Annals - Manufacturing Technology*, **60**(1), pp. 303-306.
- [26] Rasp, W., and Wichern, C. M., 2002, "Effects of Surface-Topography Directionality and Lubrication Condition on Frictional Behaviour during Plastic Deformation," *Journal of Materials Processing Technology*, **125/126**(3), pp. 379.
- [27] Stahlmann, J., Nicodemus, E. R., and Sharma, S. C., 2012, "Surface Roughness Evolution in FEA Simulations of Bulk Metal Forming Process," *Wear*, **288**(0), pp. 78-87.
- [28] Behrens, B., 2008, "Finite Element Analysis of Die Wear in Hot Forging Processes," *CIRP Annals - Manufacturing Technology*, **57**(1), pp. 305-308.
- [29] Hunter, M. S., and Fowle, P., 1956, "Natural and Thermally Formed Oxide Films on Aluminum," *Journal of the Electrochemical Society*, **103**(9), pp. 482-485.
- [30] Lenard, J. G., and Munther, P. A., 1999, "The Effect of Scaling on Interfacial Friction in Hot Rolling of Steels," *Journal of Materials Processing Technology*, **88**, pp. 105-113.
- [31] Wang, L., He, Y., and Zhou, J., 2010, "Effect of Temperature on the Frictional Behaviour of an Aluminium Alloy Sliding Against Steel during Ball-on-Disc Tests," *Tribology International*, **43**(1-2), pp. 299-306.
- [32] Pujante, J., Pelcastre, L., and Vilaseca, M., 2013, "Investigations into Wear and Galling Mechanism of Aluminium Alloy-Tool Steel Tribopair at Different Temperatures," *Wear*, **308**(1-2), pp. 193-198.

8. Appendices

Appendix A - Cigar Test Results Examining part orientation with respect to material flow without lubricant

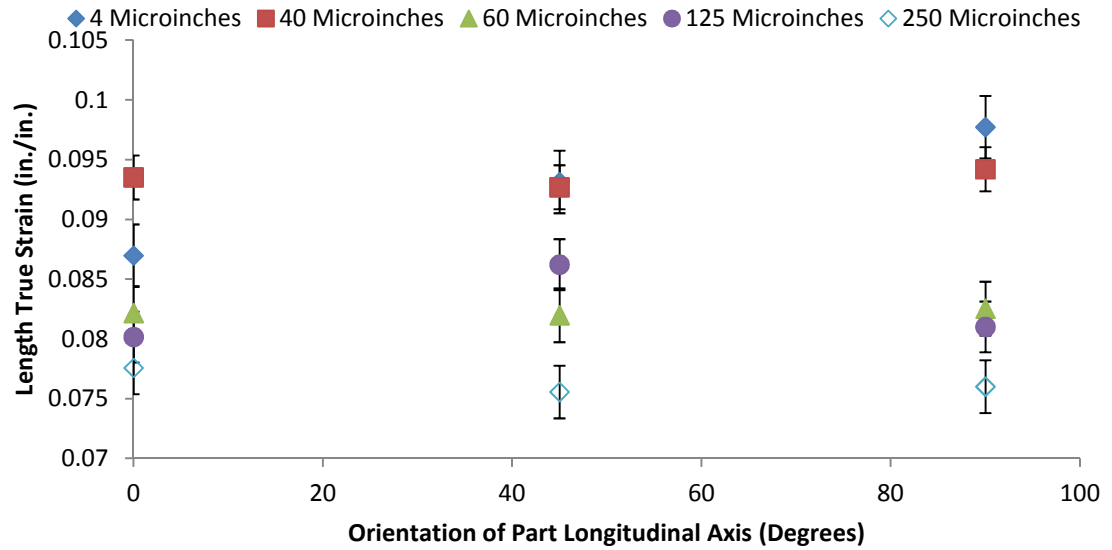


Figure 8.1 – Combined length true strain plotted as a function of part orientation in the dry state.

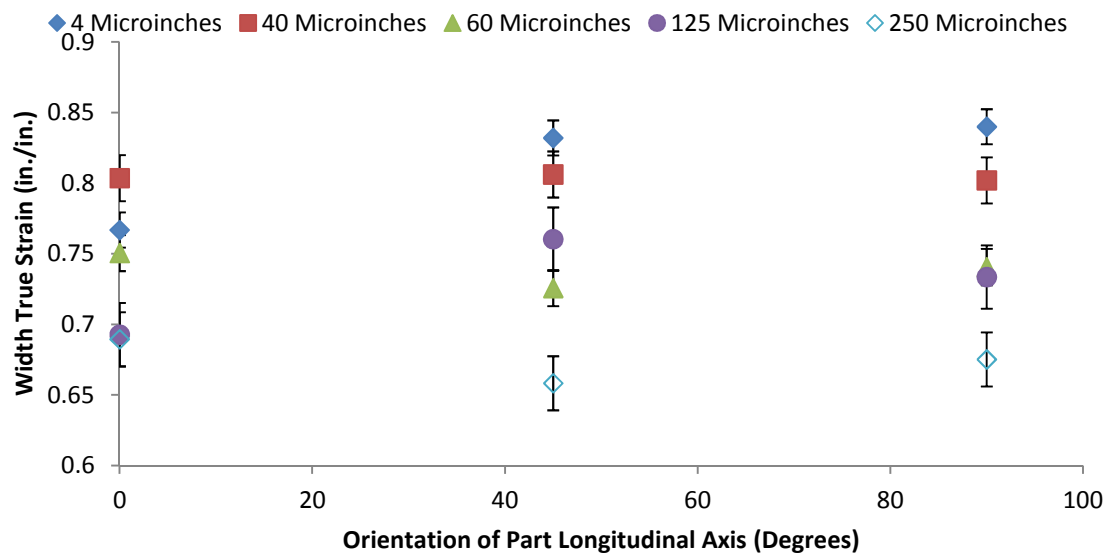


Figure 8.2 - Combined width true strain plotted as a function of part orientation in the dry state.

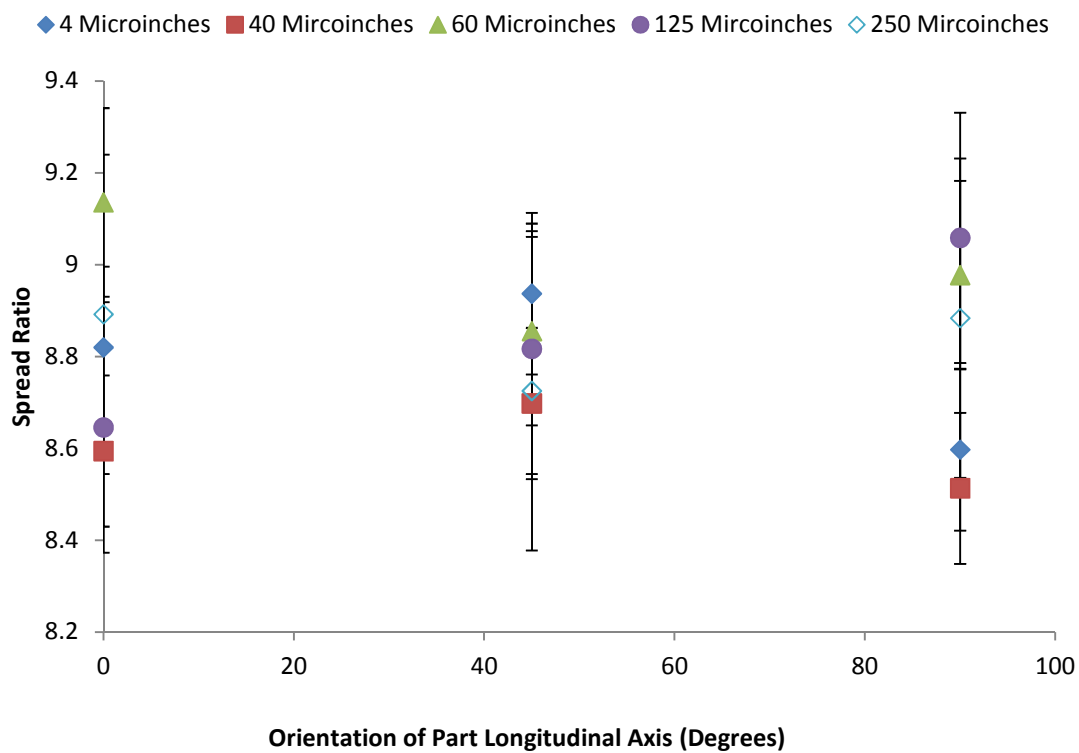


Figure 8.3 - Combined spread ratio plotted as a function of part orientation in the dry state

Appendix B - Cigar Test Results Examining Surface Roughness with respect to material flow with lubricant

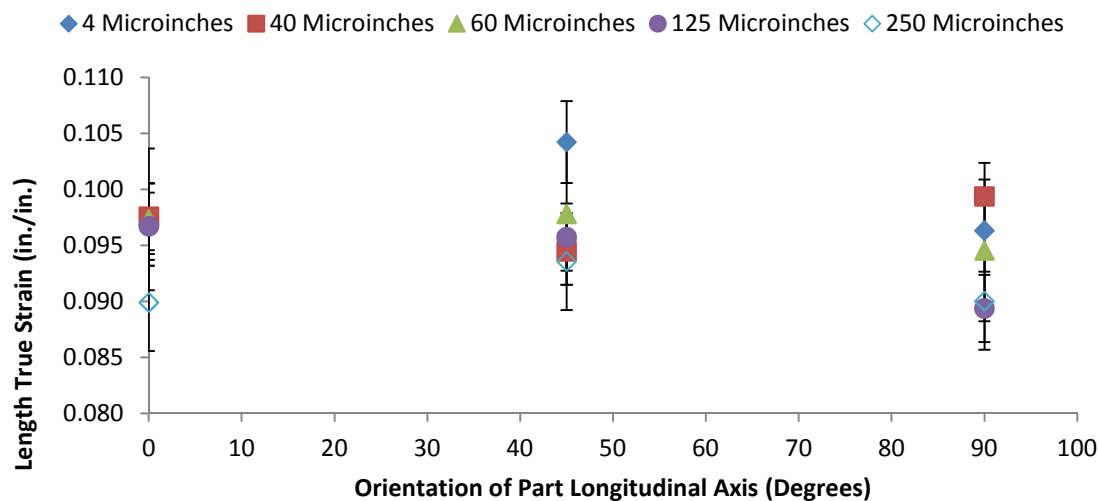


Figure 8.4 - Combined length true strain plotted as a function of part orientation completed with lubricant.

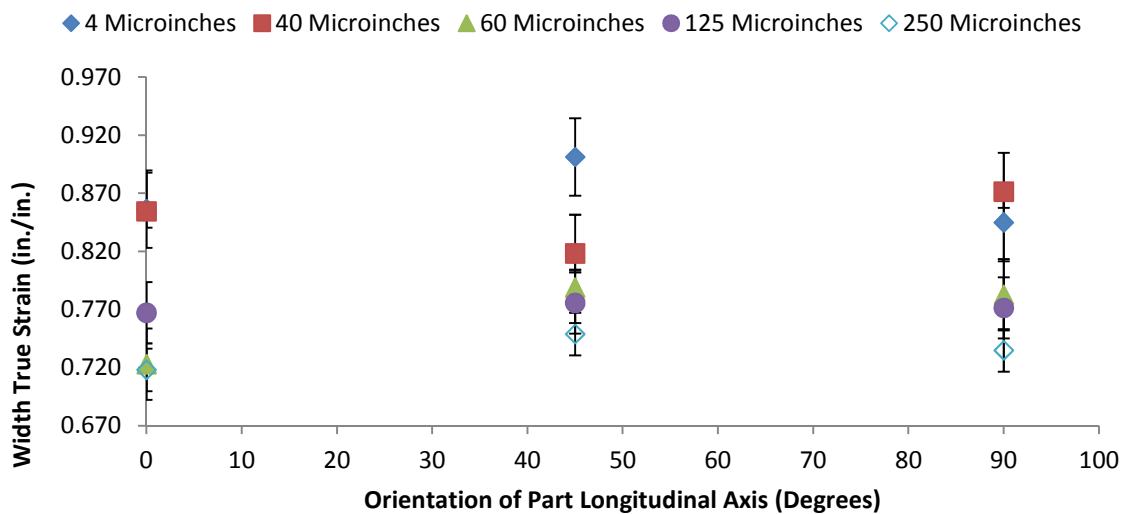


Figure 8.5 – Combined width true strain plotted as a function of part orientation completed with lubricant.

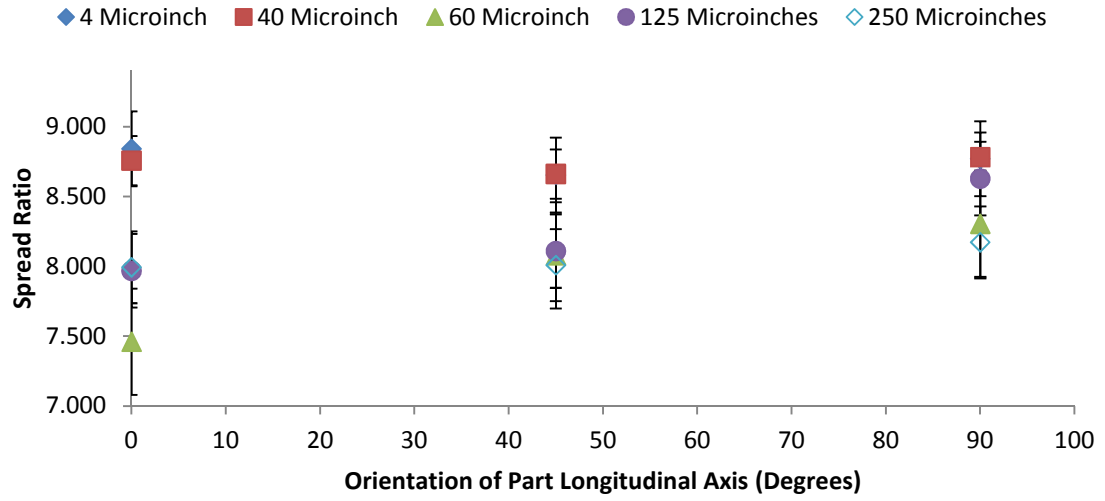


Figure 8.6 – Combined spread ratio plotted as a function of part orientation completed with lubricant.

Appendix C Calculated Standard Deviations for the Collected Data

Table 5 - Calculated sample standard deviation for each trial of the study.

Die Surface Roughness, Ra (μin)	Orientation (Degrees)	Width True Strain (in/in)		Length True Strain (in/in)		Spread Ratio	
		Dry	Lube	Dry	Lube	Dry	Lube
4	0	0.015	0.049	0.003	0.003	0.145	0.419
	45	0.003	0.025	0.002	0.005	0.213	0.293
	90	0.020	0.026	0.003	0.003	0.171	0.093
40	0	0.029	0.019	0.003	0.002	0.237	0.061
	45	0.016	0.012	0.002	0.002	0.110	0.110
	90	0.015	0.011	0.001	0.005	0.147	0.358
60	0	0.017	0.010	0.003	0.004	0.120	0.329
	45	0.004	0.022	0.002	0.004	0.214	0.441
	90	0.017	0.060	0.002	0.011	0.282	0.336
125	0	0.010	0.025	0.002	0.003	0.300	0.256
	45	0.026	0.023	0.001	0.004	0.229	0.332
	90	0.031	0.031	0.003	0.002	0.289	0.202
250	0	0.022	0.018	0.002	0.004	0.395	0.205
	45	0.017	0.021	0.004	0.004	0.383	0.209
	90	0.018	0.014	0.001	0.003	0.264	0.358